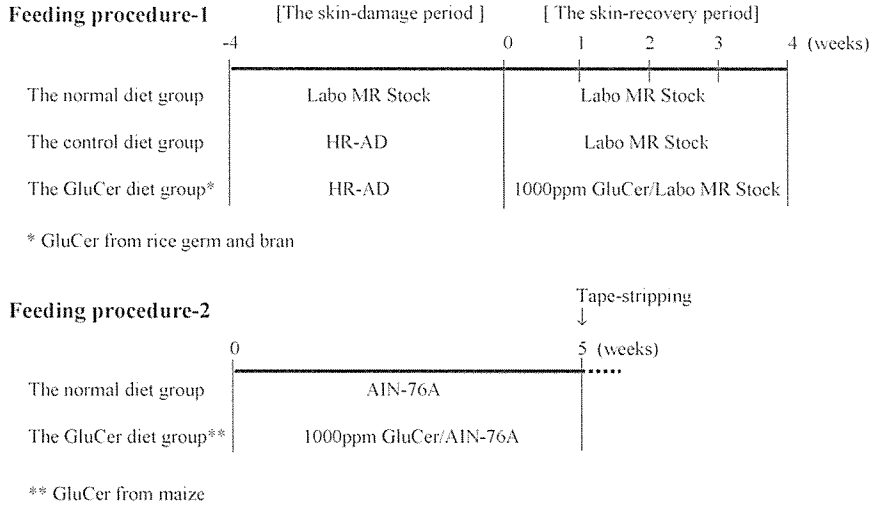

Fig. 1 Perturbation process. Feeding procedure-1: three groups (the normal diet group, the control diet group and the GluCe diet group) of hairless mice were fed a normal diet (Labo MR stock) or a special diet (HR-AD), which is known to induce skin damage, during the skin-damage period of 4 weeks. Subsequently, in the 4-week recovery period mice were fed Labo MR stock with or without GluCer (from rice). Feeding procedure-2: two groups (the normal diet group, the GluCe diet group) of hairless mice were fed a normal diet (AIN-76A) with or without GluCer (from maize) during 5 weeks. At 5 weeks, a patch of stratum corneum was removed from the dorsal skin of each mouse by stripping with adhesive tape repeatedly for five times.

Warrington, PA, USA), or an Evaporimeter AS-TW1 (Asahi Biomed, Yokohama, Japan), in accordance with the ventilated chamber method [13]. Stratum corneum flexibility was calculated by dividing the hydration measurement by the thickness of the stratum corneum, these hydration and thickness were measured by using a Corneometer ASA-M2 (Asahi Biomed, Yokohama, Japan) [13].

2.5. Chronic barrier perturbation studies

Four-week-old male hairless mice (HR-1) were randomly allocated to three groups: the normal diet group, the control diet group, and the GluCer diet group (Fig. 1, Feeding procedure-1). During the skin-damage period of 4 weeks mice were fed HR-AD or Labo MR stock diet. Subsequently, in the 4-week recovery period mice were fed Labo MR stock with or without GluCer (from rice). Food and water were provided ad libitum. TEWL or stratum corneum flexibility were measured using an Evaporimeter AS-TW1 or a Corneometer ASA-M2 (Asahi Biomed, Yokohama, Japan).

2.6. Acute barrier perturbation studies

Eight-week-old female hairless mice (Hr/Hr) were fed the AIN-76A rodent diet with or without 1000 ppm GluCer (from maize). After 5 weeks of feeding (Fig. 1, Feeding procedure-2), a patch of stratum corneum was removed from the dorsal skin of each mouse by stripping with adhesive tape (PPS Nichiban: 2.5 cm × 3.0 cm) repeatedly for five times. Before tape-stripping, TEWL was measured by using an Electrolytic water analyzer (Meeco, Warrington, PA, USA). Subsequently, immediately and 2 h after tape-stripping, TEWL was measured on the surface of tape-stripped and non-perturbed skin (as basal TEWL).

2.7. Statistics

Results were expressed as the mean ± S.D. for each group. Statistical analysis were performed using a unpaired Student's *t*-test. Statistical significance was defined as $p < 0.05$, 0.01, and 0.001.

3. Results

3.1. Effect of dietary GluCer on TEWL in hairless mice with chronic barrier perturbation

A feeding study was performed to determine the influence of GluCer (from rice) on epidermal barrier function in vivo. To induce a model of chronic barrier perturbation in skin, hairless mice were fed an HR-AD for 4 weeks (Fig. 1, Feeding procedure-1, skin-damage period); normal controls were fed a normal diet (Labo MR stock). After the skin-damage period, the mice were fed an experimental diet containing 1000 ppm GluCer (from rice) or a normal diet for 4 weeks (Fig. 1,

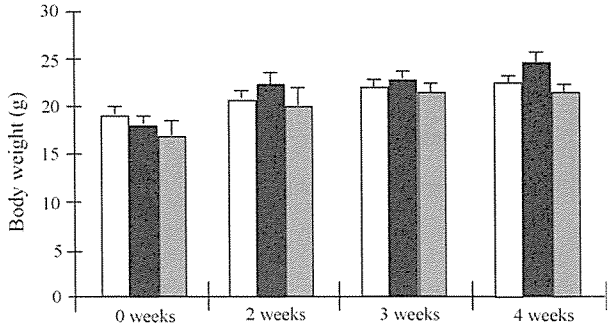

Fig. 2 Body weights of mice in the skin-recovery period. Hairless mice were fed a normal diet (Labo MR stock) or a special diet (HR-AD) for 4 weeks. Subsequently, mice were fed Labo MR stock with GluCer (the GluCer diet group) or without (the normal diet group and the control diet group), as illustrated in Fig. 1 (Feeding procedure-1). At weeks 0, 2, 3, and 4 of the skin-recovery period, the body weight of each mouse in the normal (open column), the control (black column), and HR-AD GluCer (grey column) diet groups was measured. Each column represents the mean ± S.D. of four or five animals.

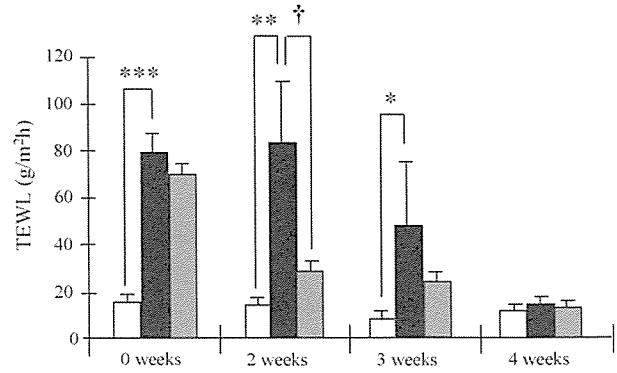

Fig. 3 Effect of dietary GluCer on transepidermal water loss (TEWL) in hairless mice with chronic barrier perturbation. Hairless mice were fed a normal diet (Labo MR stock) or a special diet (HR-AD) for 4 weeks. Subsequently, mice were fed a diet of Labo MR stock with GluCer (the GluCer diet group) or without (the normal diet group and the control diet group), as illustrated in Fig. 1 (Feeding procedure-1). At 0, 2, 3, and 4 weeks of the skin-recovery period, the TEWL was measured in each mouse of the normal (open column), the control (black column), the GluCer (grey column) diet groups using an Evaporimeter AS-TW1. Each column represents the mean ± S.D. of four or five animals. $^{*}p < 0.05$, $^{**}p < 0.01$ and $^{***}p < 0.001$. $^{\dagger}p < 0.05$.

Feeding procedure-1, the skin-recovery period). During the skin-recovery period, there were no significant differences in body weights among the three groups (Fig. 2).

We first determined the TEWL as a marker of epidermal barrier function, measured using an Evaporimeter AS-TW1 (Asahi Biomed, Yokohama, Japan), at 0, 2, 3, and 4 weeks of the skin-recovery period. In the normal diet group, the TEWL was approximately 12 g/(m^2 h) throughout the skin-recovery period (Fig. 3). In mice fed the HR-AD, the TEWL markedly increased to approximately 74.0 g/(m^2 h) by the end of the skin-damage period (0 weeks). Two weeks into the skin-recovery period, the TEWL of the control HR-AD group had not changed, but the TEWL of the GluCer diet group was significantly decreased (Fig. 3). By 3 weeks the TEWL in the GluCer group still had a tendency to be reduced compared to the control diet. These results demonstrate that the oral administration of GluCer can significantly improve the barrier function of skin affected by chronic perturbation.

3.2. Effect of dietary GluCer on stratum corneum flexibility in hairless mice

Next, we examined the effect of the diet on the stratum corneum flexibility, measured using a Corneometer ASA-M2 (Asahi Biomed, Yokohama, Japan). At the end of the skin-damage period (0 weeks) (Fig. 1, Feeding procedure-1), the flexibility was significantly reduced in the groups fed the HR-AD compared with those consuming the normal diet group (Fig. 4). Three weeks into the skin-recovery period, the GluCer diet group showed significantly increased stratum corneum flexibility compared with that of the control diet group, and nearly equal to that of the normal diet group. These results indicate that the oral administration

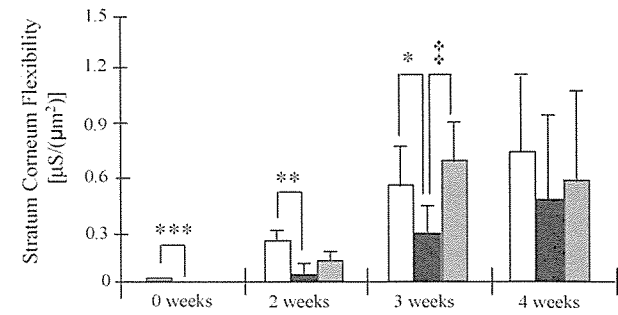

Fig. 4 Effect of dietary GluCer on stratum corneum flexibility in hairless mice with chronic barrier perturbation. Hairless mice were fed a normal diet (Labo MR stock) or a special diet (HR-AD) for 4 weeks. Subsequently, mice were fed Labo MR stock with GluCer (the GluCer diet group) or without (the normal diet group and the control diet group), as illustrated in Fig. 1 (Feeding procedure-1). At 0, 2, 3, and 4 weeks of the skin-recovery period, the stratum corneum flexibility was measured for each mouse in the normal (open column), the control (black column), and the GluCer (grey column) diet groups. Each column represents the mean ± S.D. of four or five animals. $^{*}p < 0.05$, $^{**}p < 0.01$ and $^{***}p < 0.001$. $^{\ddagger}p < 0.01$.

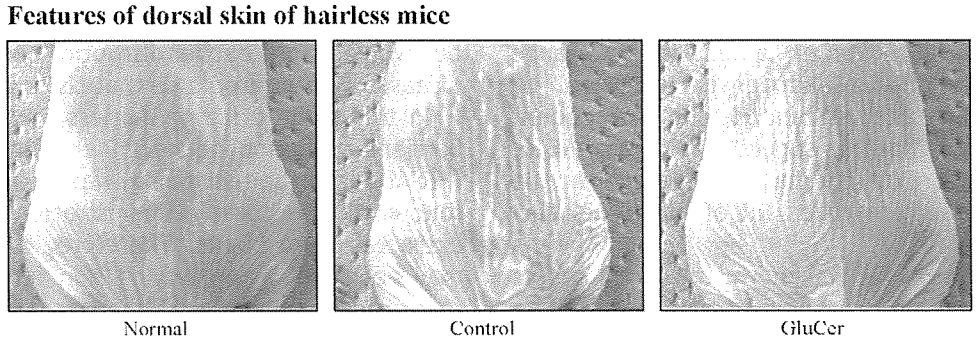

Fig. 5 Effect of dietary GluCer on skin appearance in hairless mice with chronic barrier perturbation. Hairless mice were fed a normal diet (Labo MR stock) or a special diet (HR-AD) for 4 weeks. Subsequently, mice were fed Labo MR stock with GluCer (the GluCer diet group) or without (the normal diet group and the control diet group), as illustrated in Fig. 1 (Feeding procedure-1). At 3 weeks of the skin-recovery period, the dorsal skins in a mouse of the normal diet group (left panel), the control diet group (middle panel), or the GluCer diet group (right panel) were photographed.

of GluCer can significantly elevate stratum corneum flexibility in skin with induced chronic perturbation.

3.3. Effect of dietary GluCer on skin appearance in hairless mice

At 3 weeks of the skin-recovery period (Fig. 1, Feeding procedure-1), the dorsal skin of mice from each of the three diet groups was examined (Fig. 5). The dorsal skin of the GluCer diet group showed reduced skin creases compared to creases in the control diet group, similar to skin of the normal diet group. The appearance of the dorsal skin revealed that the oral administration of GluCer reduced the number of skin creases.

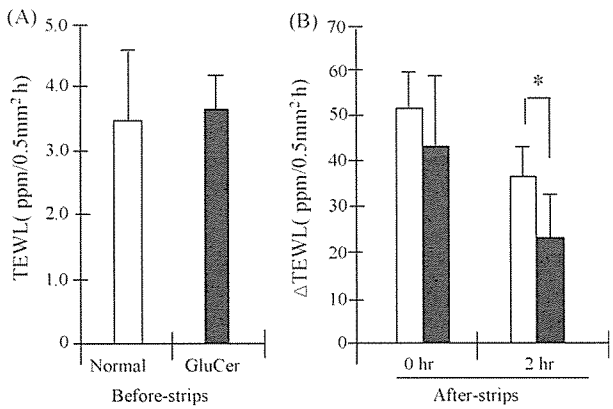

Fig. 6 Effect of dietary GluCer on the protection and recovery from acute barrier perturbation. (A) At the end of oral administration of GluCer (from maize) for 5 weeks, the TEWL were measured using a Meeco electrolytic water analyzer. (B) Following the feeding procedure in (A), the dorsal skin of each mouse was tape-stripped five times to perturb the skin barrier function. Immediately after tape-stripping (0 h) and 2 h later, the TEWL was measured in areas of perturbed and non-perturbed skin and the difference (ΔTEWL) was calculated for each mouse of the normal (open column) and GluCer (solid column) diet groups. Each column represents the mean ± S.D. of eight animals. $^{*}p < 0.05$.

3.4. Effect of dietary GluCer on recovery following acute barrier perturbation

To confirm the effect of orally administered GluCer in epidermal barrier function, we analyzed a second type of skin damage, acute perturbation. Eight-week-old female hairless mice (Hr/Hr) were fed an AIN-76A diet with or without 1000 ppm GluCer from maize (Fig. 1, Feeding procedure-2). After 5 weeks (before tape-stripping), no significant difference was observed in the TEWL of the two diet groups (Fig. 6A). To perturb the epidermal barrier function, patches of dorsal skin of each mouse were tape-stripped five times. Immediately after tape-stripping (0 h) and 2 h later, the TEWL was measured for areas of perturbed and non-perturbed skin, and the difference (ΔTEWL) was calculated for each mouse. Two hours after the damage, the difference in the ΔTEWL was significantly less in the GluCer (from maize) diet group compared with that in the normal group (Fig. 6B). This result indicated that the oral administration of GluCer accelerated recovery from acute barrier perturbation.

4. Discussion

In hairless mice with skin damage, oral administration of GluCer appeared to aid in the improvement of epidermal barrier function that had been reduced by chronic or acute perturbation. Mice fed a special skin-damaging diet (the HR-AD) exhibited increased TEWL and reduced stratum corneum flexibility. The declined skin functions improved

in mice fed a diet supplemented with GluCer. In addition, dietary GluCer aided in resistance against acute physical barrier perturbation, by tape-stripping, and enhanced the subsequent recovery. These findings suggest that dietary GluCer from plant extracts may be effective in the maintenance and improvement of epidermal barrier function.

Mice fed an HR-AD are known to exhibit atopic dermatitis-like skin symptoms, accompanied with a decline in epidermal barrier functions. Although the causative mechanism is not clear, previous reports have suggested that a dietary deficiency of some kind, perhaps in magnesium or zinc, may be involved [6]. Our study indicates that a diet supplemented with GluCer can enhance the recovery of epidermal barrier perturbation induced by an HR-AD. This finding suggests that a deficiency in GluCer might contribute to the induction of atopic dermatitis-like skin symptoms in HR-AD-fed mice. The GluCer from fungi are known to show a characteristic fungal consensus structure [11]. And then, We are investigating the effect of GluCer from tamogitake mushroom (edible fungus) on skin barrier function. In preliminary data, the application of this GluCer improved the skin-damage.

Sphingolipids, which contain ceramide and GluCer, are important constituents of the plasma membrane in mammalian cells. Sphingolipids are known to be fundamental components of the lamellar structure that mediates the epidermal permeability barrier function and skin homeostasis [14–17]. Kono et al. [18] reported that dietary sphingolipids are degraded on the brush border membrane of the small intestine, and are then taken up by enterocytes. In mice engineered with a skin-targeted conditional knockout of serine palmitoyltransferase, the enzyme responsible for the first step of sphingolipid biosynthesis, the sphingolipid composition was reportedly normal [19]. Moreover, we demonstrated that keratinocytes utilize exogenous sphingolipids to construct their own sphingolipid compositions [20]. Hence, dietary sphingolipids may be degraded and incorporated intracellularly, and used in the composition of the lamellar lipids in skin.

Upon such stimuli as exposure to ultraviolet radiation on dorsal skin or the stress of overcrowding, the TEWL of these mice is increased and the metabolism of ceramidein the epidermis is altered [21,22]. In several skin diseases a disturbance in ceramide metabolism supposedly influences skin barrier functions. In patients with atopic dermatitis or psoriasis, decreased ceramide levels and increased TEWL were observed in the lesional stratum corneum [1,23,24]. These observations suggest that a deficiency in ceramide in the epidermis might be involved in the barrier disruption observed in skin diseases such as atopic dermatitis or psoriasis.

In this study utilizing hairless mice, epidermal barrier dysfunction induced by a skin-damaging diet (HR-AD) or by tape-stripping, was shown to improve following the oral administration of GluCer extracted from plants. Therefore, dietary GluCer may be useful in preserving skin function and in recovering from epidermal barrier perturbation.

References

[1] Goldstein AM, Abramovits W. Ceramides and the stratum corneum: structure, function, and new methods to promote repair. Int J Dermatol 2003;42:256–9.
[2] Imokawa G, Abe A, Jin K, Higaki Y, Kawashima M, Hidano A. Decreased level of ceramides in stratum corneum of atopic dermatitis: an etiologic factor in atopic dry skin? J Invest Dermatol 1991;96:523–6.
[3] Di Nardo A, Wertz P, Giannetti A, Seidenari S. Ceramide and cholesterol composition of the skin of patients with atopic dermatitis. Acta Derm Venereol 1998;78:27–30.
[4] Murata Y, Ogata J, Higaki Y, Kawashima M, Yada Y, Higuchi K, et al. Abnormal expression of sphingomyelin acylase in atopic dermatitis: an etiologic factor for ceramide deficiency? J Invest Dermatol 1996;106:1242–9.
[5] Fujii M, Tomozawa J, Mizutani N, Nabe T, Danno K, Kohno S. Atopic dermatitis-like pruritic skin inflammation caused by feeding a special diet to hr-1 hairless mice. Exp Dermatol 2005;14:460–8.
[6] Makiura M, Akamatsu H, Akita H, Yagami A, Shimizu Y, Eiro H, et al. Atopic dermatitis-like symptoms in HR-1 hairless mice fed a diet low in magnesium and zinc. J Int Med Res 2004;32:392–9.
[7] Loden M, Barany E. Skin-identical lipids versus petrolatum in the treatment of tape-stripped and detergent-perturbed human skin. Acta Derm Venereol 2000;80:412–5.
[8] Schmuth M, Haqq CM, Cairns WJ, Holder JC, Dorsam S, Chang S, et al. Peroxisome proliferator-activated receptor (PPAR)-beta/delta stimulates differentiation and lipid accumulation in keratinocytes. J Invest Dermatol 2004;122:971–83.
[9] Fujino Y, Ohnishi M, Ito S. Molecular species of ceramide and mono-, di-, tri-, and tetraglycosylceramide in bran and endosperm of rice grains. Agric Biol Chem 1985;49: 2753–62.
[10] Bohn M, Heinz E, Luthje S. Lipid composition and fluidity of plasma membranes isolated from corn (Zea mays L.) roots. Arch Biochem Biophys 2001;387:35–40.
[11] Warnecke D, Heinz E. Recently discovered functions of glucosylceramides in plants and fungi. Cell Mol Life Sci 2003;60:919–41.
[12] Fukunaga K, Yoshida M, Nakajima F, Uematsu R, Hara M, Inoue S, et al. Design, synthesis, and evaluation of beta-galactosylceramide mimics promoting beta-glucocerebrosidase activity in keratinocytes. Bioorg Med Chem Lett 2003;10:813–5.
[13] Tomita Y, Akiyama M, Shimizu H. Stratum corneum hydration and flexibility are useful parameters to indicate clinical severity of congenital ichthyosis. Exp Dermatol 2005;14: 619–24.
[14] Hamanaka S, Hara M, Nishio H, Otsuka F, Suzuki A, Uchida Y. Human epidermal glucosylceramides are major precursors

of stratum corneum ceramides. J Invest Dermatol 2002;119:416–23.
[15] Hamanaka S, Nakazawa S, Yamanaka M, Uchida Y, Otsuka F. Glucosylceramide accumulates preferentially in lamellar bodies in differentiated keratinocytes. Br J Dermatol 2005;152:426–34.
[16] Genji I, Kuno H, Kawai M. Stratum corneum lipids serve as a bound-water modulator. J Invest Dermatol 1991;96: 845–51.
[17] Uchida Y, Hara M, Nishio H, Sidransky E, Inoue S, Otsuka F, et al. Epidermal sphingomyelins are precursors for selected stratum corneum ceramides. J Lipid Res 2000;41:2071–82.
[18] Kono M, Dreier JL, Ellis JM, Allende ML, Kalkofen DN, Sanders KM, et al. Neutral ceramidase encoded by the Asah2 gene is essential for the intestinal degradation of sphingolipids. J Biol Chem; in press.
[19] Osuka S, Sano S, Tojo H, Sakamoto M, Ito M, Kondoh G, et al. The role of de novo sphingolipid biosynthesis within epidermal keratinocytes in generation of lamellar bodies and barrier function of stratum corneum. Seikagaku 2003;75: 1056.
[20] Takeda S, Mitsutake S, Tsuji K, Igarashi Y. Apoptosis occurs via the ceramide recycling pathway in human HaCaT keratinocytes. J Biochem 2006;139:255–62.
[21] Takagi Y, Nakagawa H, Yaginuma T, Takema Y, Imokawa G. An accumulation of glucosylceramide in the stratum corneum due to attenuated activity of beta-glucocerebrosidase is associated with the early phase of UVB-induced alteration in cutaneous barrier function. Arch Dermatol Res 2005;297: 18–25.
[22] Aioi A, Okuda M, Matsui M, Tonogaito H, Hamada K. Effect of high population density environment on skin barrier function in mice. J Dermatol Sci 2001;25:189–97.
[23] Hara J, Higuchi K, Okamoto R, Kawashima M, Imokawa G. High-expression of sphingomyelin deacylase is an important determinant of ceramide deficiency leading to barrier disruption in atopic dermatitis. J Invest Dermatol 2000;115: 406–13.
[24] Alessandrini F, Pfister S, Kremmer E, Gerber JK, Ring J, Behrendt H. Alterations of glucosylceramide-beta-glucosidase levels in the skin of patients with psoriasis vulgaris. J Invest Dermatol 2004;123:1030–6.

doi: 10.1111/j.1365-2230.2006.02066.x

Development of lichen planus and psoriasis on lesions of vitiligo vulgaris

H. Ujiie, D. Sawamura and H. Shimizu

Department of Dermatology, Hokkaido University Graduate School of Medicine, Sapporo, Japan

Summary

This paper reports a unique case of coexistence of vitiligo vulgaris, lichen planus and psoriasis vulgaris in a 53-year-old man. Five years after the onset of vitiligo, lichen planus developed on his lower lip. Another 4 years after the onset of lichen planus, he also exhibited psoriasis on his upper arms and trunk. Both the lichen planus and psoriasis occurred on lesions of the preceding vitiligo vulgaris. We discuss potential mechanisms for association of these three dermatoses, including Koebner phenomenon and photodamage.

Vilitigo vulgaris (VV), lichen planus (LP) and psoriasis vulgaris (PV) are common skin disorders, and the coexistence of two of these three dermatoses has been previously reported, and the aetiology postulated.[1–8] Furthermore, anatomical colocalization of vitiligo and psoriasis[1–4] or LP[5–7] is frequently seen in patients. We report a unique case with coexistence of LP and PV, which developed on lesions of preceding VV. To our knowledge, this is the first report describing the development of these three skin disorders in one patient. We do not believe that this association is coincidence, as the frequency of these disorders, particularly psoriasis, in Japan is far lower than in Western countries (prevalence of psoriasis in Japanese 0.025%;[9] in whites 2.84%[10]). In addition, the anatomical colocalization supports the notion that the association is not accidental. We consider there may be some potent mechanism behind this unique case.

Report

A 53-year-old man presented with a 15-year history of multiple depigmented macules on the extremities, trunk, lips and perioral area, which had been diagnosed as VV in another clinic. Five years after the onset of this vitiligo, he also exhibited a violaceous-coloured, slightly atrophic, scaly plaque on the depigmented macule of his lower lip (Fig. 1a), which histologically showed hyperkeratosis, focal hypergranulosis, saw-tooth appearance of the epidermis, vacuolations of the basal layer, Civatte bodies and band-like lymphocytic infiltration in the superficial dermis. A diagnosis of LP was made (Fig. 2a,b). A Masson–Fontana stain showed a marked decrease in number of melanocytes in the basal layer, confirming the coexistence of vitiligo and LP in the same area. There was no evidence of LP elsewhere, such as on the oral mucosa, skin and genitalia. Another 4 years after the onset of LP, the patient also developed scaly erythematous plaques confined within the vitiliginous lesions on his upper arms and trunk (Fig. 1b,c). During his clinical course, we could not find psoriatic lesions on predisposing sites including the scalp, elbows, or knees. Skin biopsy from one of the plaques showed epidermal regular acanthosis with hyperkeratosis, parakeratosis, and infiltrations of neutrophils into the stratum corneum and subcorneal zone, compatible with PV (Fig. 3), although the distribution of psoriatic lesions on upper arms and trunk was somewhat atypical.

The patient was taking no medication that would have caused either LP or PV, and there was no past history of sun exposure or treatment with psoralen ultraviolet A on the psoriatic lesion. Physical and laboratory examinations detected no evidence of diabetes, hepatitis C virus infection, thyroid or other autoimmune disease.

Correspondence: Dr Hideyuki Ujiie, Department of Dermatology, Hokkaido University Graduate School of Medicine, N15 W7, Kita-ku, Sapporo 060–8638, Japan.
E-mail: h-ujiie@med.hokudai.ac.jp

Conflict of interest: none declared.

Accepted for publication 16 November 2005

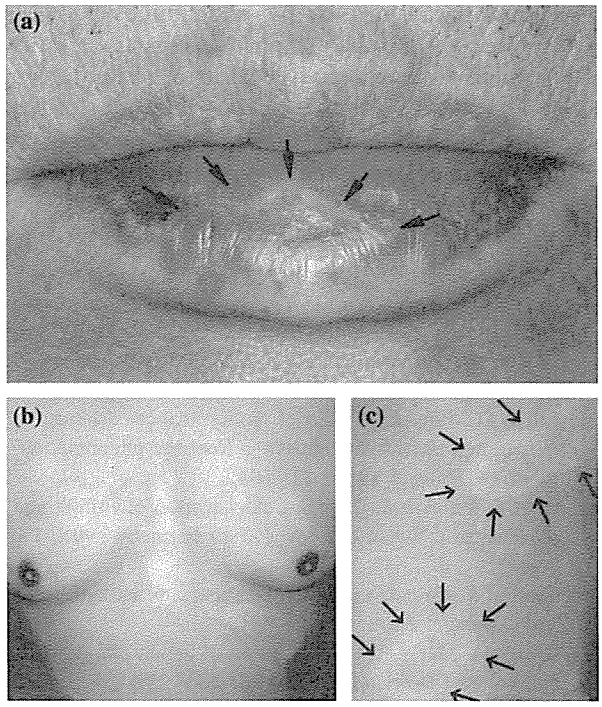

Figure 1 (a) Lichen planus on the patient's lower lip (arrows) overlaps with the macule of vitiligo on the perioral region. (b) Psoriatic plaques are limited within the vitiliginous patches on the arms, trunk. (c) Close-up view of psoriasis on the vitiliginous lesion on the right upper arm, showing glossy erythematous lesions on whitish macules (arrows).

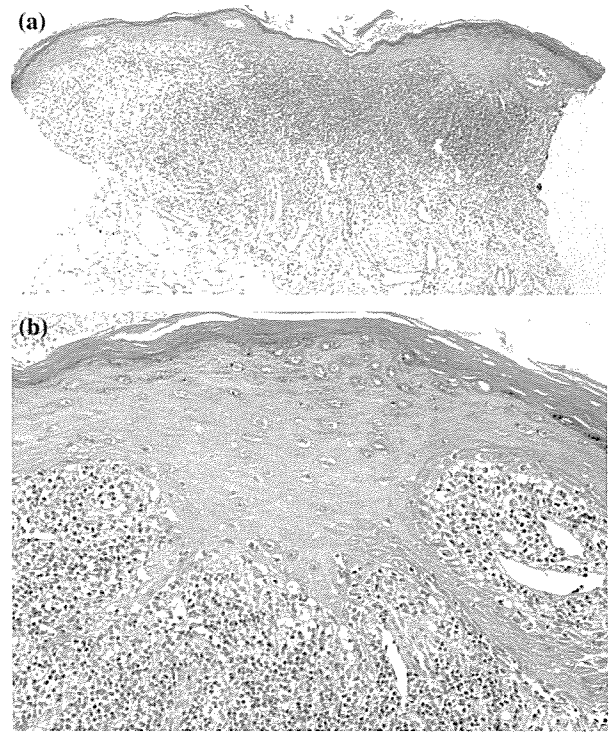

Figure 2 (a) Biopsy specimen taken from the lichen planus plaque on the lower lip, showing focal hypergranulosis and band-like lymphocytic infiltration in the superficial dermis. (b) Hyperkeratosis, focal hypergranulosis, vacuolations of the basal layer and saw-tooth appearance of the epidermis. Several Civatte bodies are also seen on the dermoepidermal junction. Haematoxylin and eosin, original magnification (a) ×40; (b) ×100.

Skin lesions of PV were resolved using topical fluocinonide and maxacalcitol ointments twice daily; however, his LP remained and the VV gradually expanded. Application of topical tacrolimus ointment twice daily to the lips resulted in the disappearance of LP. Finally, only the vitiliginous lesions remained.

VV, PV and LP are common skin conditions, considered to have an immunological component in their pathogeneses. Therefore, we presume that there is some pathogenic relationship between these dermatoses. Psoriasis and vililigo are common skin disorders, and the association of the two diseases has been well known,[1–4] usually with vitiligo preceding psoriasis.[4] The incidence of psoriasis in individuals in races with deeply pigmented skin is known to be lower than those with less pigment.[9,10] In addition, the occasional tendency of psoriatic lesions to occur on vitiliginous lesions has been reported.[1–4] This suggests that decreasing melanin might be a predisposing factor to develop psoriasis although the mechanisms of the coexistence of psoriasis and vitiligo are still unclear. In the present case, the development of psoriatic lesions only on the preceding vitiliginous lesions indicated against coincidence.

An interesting point of our case is occurrence of LP on depigmented lesions of the lips as well as PV on the vitiligous patches. Several reports have described lesions of LP being associated with those of VV, and suggest that photodamage within the vitiliginous skin may alter the expression of antigens identified by infiltrating T cells in LP.[5,7] Psoriasis and LP are well known to show Koebner phenomenon. As previous reports suggested, we also agree that some cellular injury in vitiliginous skin might lead to immune mechanisms causing Koebner phenomenon.[11] Furthermore, addition of photodamage is likely to modify expression of Koebner phenomenon, resulting in LP on sun-exposed area and PV on unexposed areas.

Wayte *et al.* reported a case of areas of long-standing vitiligo that were spared in LP.[8] They considered that in vitiliginous skin, depletion of or functional changes in Langerhans cells was the cause of the LP sparing these

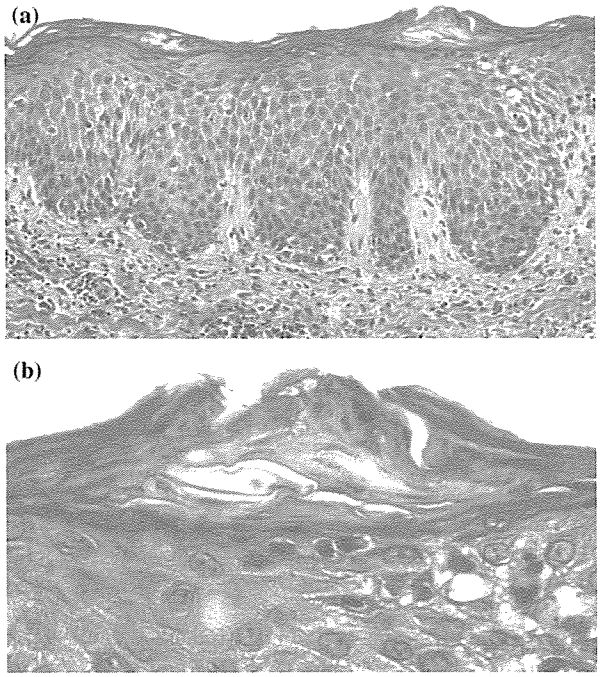

Figure 3 Skin specimen taken from the psoriasis vulgaris on the chest. (a) Epidermal regular acanthosis with hyperkeratosis and parakeratosis; (b) hyperkeratosis and parakeratosis with the infiltrations of some neutrophils into the stratum corneum and subcorneal zone. Haematoxylin and eosin, original magnification (a) ×100; (b) ×400.

areas. In addition, they discussed alteration in antigenicity of keratinocytes surrounding but not occurring within vitiligo lesions, and UV-induced immunosuppression that was marked in skin lacking photoprotective pigment. In contrast, in our case, numerous infiltrations of lymphocytes found in the specimen of our LP on the patient's lower lip represent a distinct inflammatory reaction causing LP only within the vitiliginous skin. It may be that no immunosuppressive reaction occurred in the vitiliginous areas in our case.

We report the first case of coexistence of VV, LP and PV in a single individual. The pathogenesis is unclear in this case, but we consider that Koebner phenomenon related to photodamage could explain this rare coexistence of three dermatoses.

References

1 Menter A, Boyd AS, Silverman AK. Guttate psoriasis and vitiligo: anatomic cohabitation. *J Am Acad Dermatol* 1989; **20**: 698–700.
2 Julian CG, Bowers PW. Strict anatomical coexistence of vitiligo and psoriasis vulgaris – a Koebner phenomenon? *Clin Exp Dermatol* 1996; **21**: 464.
3 Dhar S, Malakar S, Dhar S. Colocalization of vitiligo and psoriasis in a 9-year-old boy. *Pediatr Dermatol* 1998; **15**: 242–3.
4 Sandhu K, Kaur I, Kumar B. Psoriasis and vitiligo. *J Am Acad Dermatol* 2004; **51**: 149–50.
5 Anstey A, Marks R. Colocalization of lichen planus and vitiligo. *Br J Dermatol* 1993; **128**: 103–4.
6 Baran R, Ortonne JP, Perrin C. Vitiligo associated with a lichen planus border. *Dermatology* 1997; **194**: 199.
7 Sardana K, Sharma RC, Koranne RV *et al.* An interesting case of colocalization of segmental lichen planus and vitiligo in a 14-year-old boy. *Int J Dermatol* 2002; **41**: 508–9.
8 Wyte J, Wilkinson JD. Unilateral lichen planus, sparing vitiliginous skin. *Br J Dermatol* 1995; **133**: 817–18.
9 Aoki T, Yoshikawa K. Psoriasis in Japan. *Arch Dermatol* 1971; **104**: 328–9.
10 Lomholt G. Psoriasis: *Prevalence, spontaneous course, and genetics. A census study on the prevalence of skin disease on the Faroe Islands.* Copenhagen: GEC Gad 1963; 31–3.
11 Papadavid E, Yu RC, Munn S, Chu AC. Strict anatomical coexistence of vitiligo and psoriasis vulgaris – a Koebner phenomenon? *Clin Exp Dermatol* 1996; **21**: 138–40.

ruled out on clinical, radiological, and pathologic findings. Treatment of lupus mastitis, which does not differ from that of lupus erythematosus profundus found in other locations, includes mainly systemic glucocorticoids and hydroxychloroquine, but in 1 case mastectomy was required because of a painful breast mass in which the pain was not controlled with glucocorticoids.[5]

Claude Bachmeyer, MD
Isabelle Goubin, MD
Hélène Berseneff, MD
Laurent Blum, MD

Correspondence: Dr Bachmeyer, Service de Médecine Interne, CHU Tenon, 4 rue de la Chine, 75020 Paris, France (claude.bachmeyer@tnn.ap-hop-paris.fr).
Financial Disclosure: None.

1. Requena L, Sanchez Yus E. Panniculitis, part II: mostly lobular panniculitis. *J Am Acad Dermatol*. 2001;45:325-361.
2. De Bandt M, Meyer O, Grossin M, Kahn MF. Lupus mastitis heralding systemic lupus erythematosus with antiphospholipid syndrome. *J Rheumatol*. 1993; 20:1217-1220.
3. Cernea SS, Kihara M, Sotto MN, Vilela MA. Lupus mastitis. *J Am Acad Dermatol*. 1993;29:343-346.
4. Holland NW, McKnight K, Challa VR, Agudelo CA. Lupus panniculitis (profundus) involving the breast: report of 2 cases and review of the literature. *J Rheumatol*. 1995;22:344-346.
5. Georgian-Smith D, Lawton TJ, Moe RE, Couser WG. Lupus mastitis: radiologic and pathologic features. *AJR Am J Roentgenol*. 2002;178:1233-1235.

Lupus Erythematosus Profundus Successfully Treated With Dapsone: Review of the Literature

Lupus erythematosus profundus (LEP) is a clinical subtype of cutaneous lupus erythematosus that has a chronic and recurrent clinical course. Systemic corticosteroids, which are often administered in cases of LEP complicated with systemic lupus erythematosus, are generally effective but cause side effects. Thus, other therapeutic options are needed. Hydroxychloroquine and thalidomide have occasionally been used as first-line therapies for LEP[1,2]; however, the sale of them is prohibited in Japan because of their severe side effects. Alternatively, dapsone has been used in Japan. Indeed, there were several case reports written in the Japanese literature describing patients with LEP successfully treated with dapsone ; however, few cases have been reported in the English literature.[3,4] Herein we report a case of LEP successfully treated with dapsone, and we review the previous Japanese cases.

Report of a Case. A 56-year-old Japanese woman presented with a 3-year history of erythema on her upper right arm. Over a 2-month period, the lesion gradually increased in size and became indurated, ulcerated, and painful. On physical examination, we found a 35 × 30-mm depressed indurated area with two 15-mm-diameter ulcers on the right upper arm (**Figure 1**A). There was no medical history of trauma to this area, of its having been an injection site, or of systemic corticosteroid therapy having been administered to this patient. A skin biopsy specimen taken from the edge of the ulcer demonstrated lobular panniculitis with an inflammatory infiltrate predominantly composed of lymphocytes and scattered plasma cells (**Figure 2**). Culture of the biopsy specimen did not yield bacteria, acid-fast bacilli, or fungi. Laboratory examination findings including complete blood cell count, liver and renal function test values, and immunoglobulin, complement, and C-reactive protein levels were all normal. The titers of antinuclear antibodies were 1:40 with a speckled pattern, but the values for anti-DNA and anti-Sm antibody were negative. From these findings, the diagnosis of LEP was made.

We administered dapsone, 75 mg/d. Surprisingly, a remission from pain was observed within several days, and the expansion of the indurated area stopped within

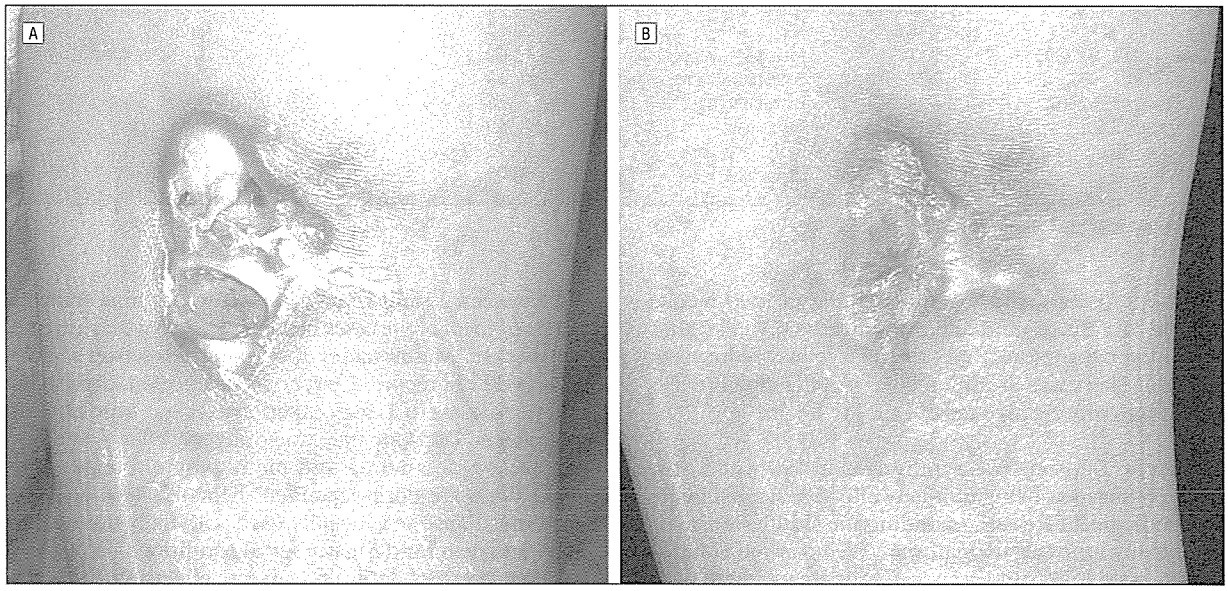

Figure 1. Clinical features of lupus erythematosus profundus on the right upper arm. A, Before treatment; B, 6 weeks after treatment with dapsone, 75 mg/d.

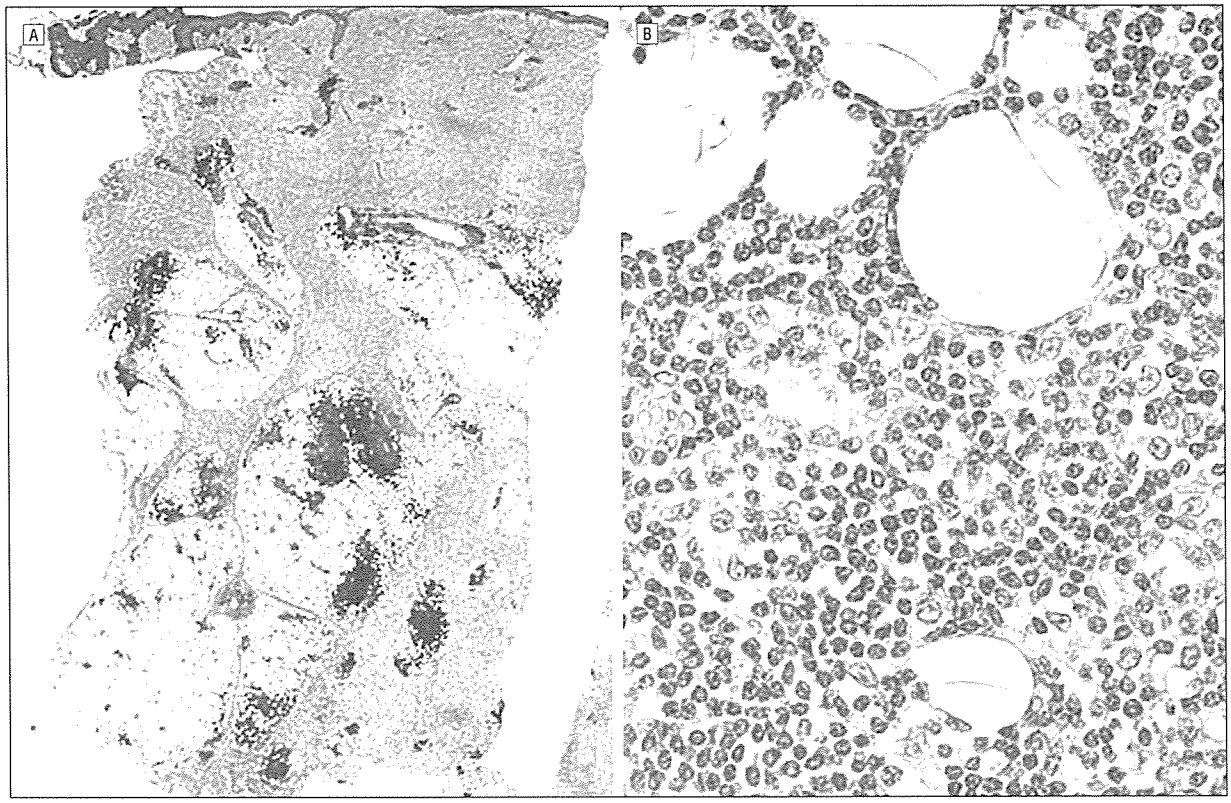

Figure 2. Hematoxylin-eosin staining of the skin specimen. A, Low-power magnification of the entire skin lesion demonstrated dense island-like inflammatory cell infiltration through the dermal to the subcutaneous fat tissue layers (original magnification ×10). B, Lobular panniculitis was mainly composed of lymphocytes intermingled with some plasma cells (original magnification ×400).

Table. Review of Cases With Lupus Erythematosus Profundus Successfully Treated With Dapsone

Source	Patient No./ Age, y/Sex	Distribution	Dosage per Day, mg	Time Until Remission, wk	Adverse Effects
Ueki et al,[6] 1989	1/36/F	Face, upper limb	75	3	No
Yamada et al,[3] 1989	2/41/M	Upper limb, thigh	75	8	No
Yasue et al,[7] 1992	3/38/F	Limbs, waist	75	NS	Drug eruption
Ishikawa et al,[8] 1994	4/45/F	NS	25-50	2	No
Yamamoto et al,[9] 1996	5/47/F	Face, neck, upper limbs	25-50	4	Headache, hypertension
Fukui et al,[10] 1998	6/21/F	Face, upper limbs, chest	50	NS	No
Oshitani et al,[11] 2000	7/33/F	Face, buttocks	75	3	No
Kai et al,[12] 2000	8/46/F	Face, waist	50	8	No
Kai et al,[12] 2000	9/36/F	Scalp, face, back	75	8	No
Present study	10/56/F	Upper limb	50-75	1	Anemia

Abbreviation: NS, not stated.

1 week. Ulcers rapidly reepithelialized in 6 weeks (Figure 1B). Since mild anemia appeared 6 weeks after beginning dapsone therapy, the dosage was reduced to 50 mg/d. There was prompt recovery of hemoglobin levels without any recurrence of LEP for 1 year.

Comment. Dapsone was synthesized in 1908, and now it is recognized as being uniquely effective against many dermatological diseases, including the skin lesions that accompany lupus erythematosus.[5] We reviewed 10 well-documented cases of LEP successfully treated with dapsone (**Table**). In our review, the initial dose of dapsone was between 25 and 75 mg/d, and disease remission was obtained in all of the cases between 1 and 8 weeks (mean: 4.6 weeks). Maintenance therapy and long-term outcome were not reported, but no recurrence was described.

The patients in 3 cases experienced some kind of mild side effects. Dapsone may cause adverse effects, including hemolytic anemia and methemoglobinemia. Because these are dose-dependent hematological adverse reactions, dapsone is usually used with daily dosages of 100 mg or less for dermatological conditions. In our experience, most of dapsone's adverse effects are preventable with appropriate monitoring of complete blood cell,

reticulocyte, and platelet counts and of the results from liver and renal function tests. When the lowering of hemoglobin levels is detected, rapid reduction of dapsone dosage usually produces a prompt recovery in hemoglobin levels.

In conclusion, the present case and the previous ones indicate that dapsone can be a choice for the treatment of LEP because this drug is a highly effective and safe treatment for LEP.

Hideyuki Ujiie, MD
Tadamichi Shimizu, MD, PhD
Miki Ito, MD
Ken Arita, MD
Hiroshi Shimizu, MD, PhD

Correspondence: Dr Ujiie, Department of Dermatology, Hokkaido University Graduate School of Medicine, N15 W7, Kita-ku, Sapporo 060-8638, Japan (h-ujiie@med.hokudai.ac.jp).
Financial Disclosure: None.
Acknowledgment: We wish to thank James R. McMillan, PhD, for his critical reading of the manuscript.

1. Fox JN, Klapman MH, Rowe L. Lupus profundus in children: treatment with hydroxychloroquine. *J Am Acad Dermatol*. 1987;16:839-844.
2. Burrows NP, Walport MJ, Hammond AH, Davey N, Jones RR. Lupus erythematosus profundus with partial C4 deficiency responding to thalidomide. *Br J Dermatol*. 1991;125:62-67.
3. Yamada Y, Dekio S, Jidoi J, Ozasa S. Lupus erythematosus profundus: report of a case treated with dapsone. *J Dermatol*. 1989;16:379-382.
4. Jakes JT, Dubois EL, Quismorio FP Jr. Antileprosy drugs and lupus erythematosus. *Ann Intern Med*. 1982;97:788.
5. Wolf R, Matz H, Orion E, Tuzun B, Tuzun Y. Dapsone. *Dermatol Online J*. 2002;8:2.
6. Ueki H, Tuda N, Ono M. Effective treatment of cutaneous lupus erythematosus with DDS (dapsone) [in Japanese]. *Nishinihon J Dermatol*. 1989; 51:478-483.
7. Yasue T, Liu D, Ohashi M. Lupus erythematosus profundus with Hashimoto disease showing atrophic blanche-like eruptions [in Japanese]. *Rinsho Derma (Tokyo)*. 1992;34:615-618.
8. Ishikawa O, Miyachi Y. Diaminodiphenyl sulfone in the treatment of patients with lupus erythematosus [in Japanese]. *Jpn J Dermatol*. 1994;104: 105-108.
9. Yamamoto T, Yoshimura M, Yamamoto S. Lupus erythematosus profundus successfully treated with dapsone [in Japanese]. *Rinsho Derma (Tokyo)*. 1996; 38:615-618.
10. Fukui M, Fujii H, Tanaka T, Miyachi Y. A case of lupus erythematosus profundus [in Japanese]. *Acta Dermatol-Kyoto*. 1998;93:575-579.
11. Oshitani Y, Nitta Y. Lupus erythematosus profundus: report of a case treated with DDS [in Japanese]. *Rinsho Derma (Tokyo)*. 2000;42:1261-1264.
12. Kai M, Tanaka M, Izumi T, Tajima S, Nishikawa T. Two cases of lupus erythematosus profundus responded to diaphenylsulfon [in Japanese]. *Jpn J Clin Dermatol*. 2000;54:129-132.

Successful Treatment of a Widespread Inflammatory Verrucous Epidermal Nevus With Etanercept

Inflammatory linear verrucous epidermal nevus (ILVEN) is an uncommon dermatosis characterized by erythematous, pruritic, inflammatory papules that occur as linear bands along the lines of Blaschko. Histologic analysis reveals epidermal psoriasiform hyperplasia with characteristic alternating orthokeratosis and parakeratosis. Lesions may be difficult to distinguish from linear psoriasis because of their clinical and histopathologic similarities.[1] Unlike psoriasis, ILVEN is typically refractory to treatment, and patients seek medical care for relief of pruritus as well as cosmetic improvement. Reported treatments include topical agents, dermabrasion, cryotherapy, laser therapy, and surgical excision. These therapies have a high failure rate because of incomplete relief of symptoms, scarring, or recurrence.[2]

Report of a Case. A 55-year-old white woman with a medical history of arthritis and osteoporosis presented with pruritic, pink, scaly plaques in the Blaschko lines on her face, trunk, and extremities. The lesions had been present since age 6 months and diagnosed as widespread inflammatory epidermal verrucous nevi by clinicopathologic correlation with 3 prior biopsy findings. Over years, the patient was prescribed several therapies including moisturizers, topical and intramuscular steroids, topical lactic acid, pimecrolimus cream, and isotretinoin. The patient noted minimal improvement with isotretinoin that lasted only until the treatment was discontinued. She had the largest reduction in pruritus with intramuscular corticosteroid injections, which improved the redness and pruritus from a score of 9 to a score of 4 or 5 on a visual analog scale of 1 to 10 (10 being the most severe).

Examination revealed diffuse erythema of the face and palms with widespread classic ILVEN on the face, trunk, and all extremities (**Figure**, A). Striae were present over the arms and legs. There was no nail involvement or obvious joint deformity.

Given the extent of disease and the limitations of further systemic corticosteroid treatment, and knowing the

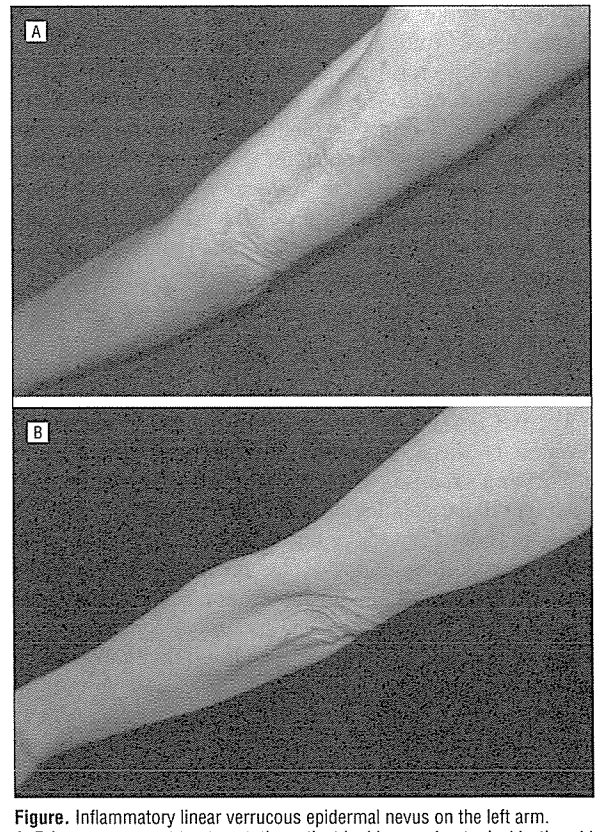

Figure. Inflammatory linear verrucous epidermal nevus on the left arm. A, Prior to etanercept treatment, the patient had been using topical lactic acid and moisturizers. B, After 6 months of etanercept therapy, there was marked improvement in roughness and erythema.

Correspondence

Severe cholinergic urticaria successfully treated with scopolamine butylbromide in addition to antihistamines

doi: 10.1111/j.1365-2230.2006.02117.x

Cholinergic urticaria is a distinctive urticarial subtype in which numerous, characteristic, small pruritic weals appear on the skin surrounded by erythema provoked by stimuli such as exercise, mild heat, bathing, eating hot or spicy foods, and emotional distress, which produce an increase in body core temperature and sweating. The majority of cholinergic urticaria reactions are mild to moderate in severity; however, a few severe cases with concomitant systemic reactions have been seen.[1] In addition, severe cholinergic urticaria sometimes resists conventional antihistamine treatment. Anticholinergic agents have been reported in the literature as an alternative therapeutic choice for cholinergic urticaria because acetylcholine, a principal mediator of sweating, has been considered to play an important role in its pathogenesis.[2,3] Here, we report a severe refractory case of cholinergic urticaria that was successfully treated with scopolamine (syn. hyoscine) butylbromide, an anticholinergic agent, in addition to antihistamines.

A 19-year-old Japanese man presented with a 6-week history of small itchy weals and erythema provoked by exercise, mild heat, and hot baths, which was occasionally associated with dizziness, cardiac palpitations, and dyspnoea. He was unable to perform even moderate exercise because of these symptoms. Provocation tests including performing exercise (with a 6-hour gap after eating before exercise challenge), hot showers and even eating spicy food easily produced a positive reaction with appearance of the same skin lesions followed by dizziness and dyspnoea. Physical examination and laboratory examination including routine haematological and blood chemistry tests were all normal. No systemic condition including cardiac, pulmonary and neurological disease was found. We diagnosed his symptoms as a severe cholinergic urticaria associated with systemic reactions. Treatment with two types of H1 blocker (hydroxyzine pamoate 25 mg and oxatomide 30 mg, twice daily) failed to relieve his symptoms, so we then added a H2 blocker (famotidine 20 mg, twice daily). As there had been no response to these treatments for a week, we started treatment with an oral anticholinergic agent (scopolamine butylbromide 10 mg, three times daily) in addition to those antihistamines, which improved his symptoms within 2 days. No systemic reactions were noted even during exercise over the next 10 months, and no adverse effect has been observed.

Severe cholinergic urticaria cases are sometimes resistant to conventional antihistamine therapy. Some types of alternative treatment have been tried, such as atropine sulphate,[2] propranolol[4] and scopolamine butylbromide.[3]

The pathogenesis of cholinergic urticaria is still not clear. Sweating associated with increased core temperature, and intracutaneous injection of cholinergic agents produce small weals in cholinergic urticaria patients.[5] These facts suggest that acetylcholine is associated with the pathogenesis of cholinergic urticaria. Therefore, we attempted oral scopolamine butylbromide treatment, which remarkably improved all the patient's cholinergic urticaria symptoms.

Systemic anticholinergic agents can cause some adverse effects such as constipation, thirst and dysfunction of accommodation of the eye. However, the treatment with scopolamine butylbromide was well tolerated by our patient. The reason may be that the dose of scopolamine butylbromide (10 mg three times daily) is in the low range in comparison with the dose for abdominal pain to suppress intestinal spasm (10–20 mg, 3–5 times daily). With caution regarding some adverse effects, a combination therapy with anticholinergic and antihistamine agents can be used as one of the therapeutic options for severe cholinergic urticaria. Other anticholinergics besides scopolamine butylbromide, e.g. probantheline bromide, are also potentially useful.

H. Ujiie, T. Shimizu, K. Natsuga, K. Arita, K. Tomizawa,* and H. Shimizu

Departments of Dermatology, Hokkaido University Graduate School of Medicine, Sapporo, Japan; and
**Ebetsu City Hospital, Ebetsu, Japan*
E-mail: h-ujiie@med.hokudai.ac.jp
Conflict of interest: none declared.
Accepted for publication 12 January 2006

References

1 Zuberbier T, Althaus C, Chantraine-Hess S *et al.* Prevalence of cholinergic urticaria in young adults. *J Am Acad Dermatol* 1994; **31**: 978–81.

2 Kobayashi H, Aiba S, Yamagishi T *et al.* Cholinergic urticaria, a new pathogenic concept: hypohidrosis due to interference with the delivery of sweat to the skin surface. *Dermatology* 2002; **204**: 173–8.
3 Tsunemi Y, Ihn H, Saeki H *et al.* Cholinergic urticaria successfully treated with scopolamine butylbromide. *Int J Dermatol* 2003; **42**: 850.
4 Ammann P, Surber E, Bertel O. Beta blocker therapy in cholinergic urticaria. *Am J Med* 1999; **107**: 191.
5 Itakura E, Urabe K, Yasumoto S *et al.* Cholinergic urticaria associated with acquired generalized hypohidrosis: report of a case and review of the literature. *Br J Dermatol* 2000; **143**: 1064–6.

Oral anticoagulants may prevent NSAID-induced urticaria

doi: 10.1111/j.1365-2230.2006.02118.x

About 30% of patients with chronic urticaria (CU) experience flares of hives and/or angio-oedema after ingesting either aspirin or nonsteroidal anti-inflammatory drugs (NSAIDs).[1] Such patients are characterized by cross-reactivity to all NSAIDs that inhibit cycloxygenase (COX)-1, which suggests a pathogenic mechanism based upon the inhibition of this enzyme.[2] However, some published studies suggest that anticoagulant therapy may also be beneficial in some cases of CU. After the first single case reports of the efficacy of warfarin therapy in patients with CU,[3,4] the effectiveness of this drug in a proportion of patients was recently established by a double-blind, placebo-controlled, cross-over study.[5] The present case report adds further evidence that, at least in some patients, anticoagulant therapy may interfere with pathogenic mechanisms involved both in spontaneous urticaria and NSAID-induced exacerbations.

A 55-year-old man was seen 5 years previously at this allergy centre for severe, acute urticaria following the ingestion of a 100-mg diclofenac tablet. This episode was controlled by intravenous antihistamines and corticosteroids administered in the emergency department. The patient had been suffering from dermographism for many years and had also experienced some slight, occasional episodes of spontaneous urticaria. All screening laboratory investigations (blood cell count, erythrocyte sedimentation rate, chemistry panel, anti-nuclear antibodies, thyroid antibodies and thyroid function) were normal. After informed written consent was obtained, oral challenges with increasing doses of alternative NSAIDs exerting little or no inhibitory effect on COX-1, including acetaminophen (total cumulative dose 500 mg), nimesulide (100 mg) and tramadol (50 mg) were carried out at this allergy centre in a single-blind, placebo-controlled fashion as previously described.[6] The patient tolerated all alternative drugs. One year later, he experienced one single episode of generalized urticaria after swimming in the sea during the summer holidays; an ice-cube test carried out 2 months later scored negative.

Some years later, the patient began experiencing atrial fibrillation and hypercoagulability, causing thrombosis in the lower limbs. Preventive anticoagulant therapy with acenocumarol 1 mg daily was started. About 6 months after starting this therapy, he attended his workplace infirmary for severe back pain, where he was inadvertently given diclofenac 200 mg intramuscularly. In view of his history, the staff immediately prepared to face a drug-induced allergic reaction but rather surprisingly the patient tolerated the drug well. At a subsequent visit to our allergy centre, the patient reported that after the start of anticoagulant therapy (which had not been stopped at any time) he no longer experienced episodes of spontaneous urticaria, and his dermographism was also markedly reduced.

This patient, with a history of long-lasting dermographism, did not meet the criteria for the diagnosis of CU, but nevertheless experienced some spontaneous episodes of acute urticaria. Both dermographism and NSAID intolerance are rather common in patients with CU, and it has been shown than NSAID intolerance might precede the onset of CU by years.[7] Oral anticoagulants inhibit the synthesis of vitamin K-dependent proteins in the clotting cascade (i.e. prothrombin, and factors VII, IX and X) acting as competitive inhibitors of the vitamin, which prevent its conversion from the inactive to the active form. The inhibition of thrombin production caused by anticoagulants also produces anti-inflammatory effects, as thrombin induces endothelial secretion of mediators (E-selectin and interleukin-8) which facilitate neutrophil activation and extravasation.[8] In a very recent cooperative study carried out at our allergy centre, virtually all patients with CU (defined as the occurrence of spontaneous weals with or without angio-oedema for more than 6 weeks) scored positive on intradermal injection of autologous plasma anticoagulated with sodium citrate and showed signs of thrombin activation.[9] Notably, only 50% of them were positive for autologous serum skin test. Normal controls were all negative for the intradermal injection of both autologous serum and plasma. It is therefore possible that warfarin and other anticoagulants downregulate some adhesion molecules that are relevant in the pathogenesis of CU and also participate in NSAID-induced exacerbations of the disease.

R. Asero
Ambulatorio di Allergologia, Clinica San Carlo, Via Ospedale 21, 20037 Paderno Dugnano (MI), Italy
E-mail: r.asero@libero.it
Conflict of interest: none declared.
Accepted for publication 12 January 2006

References

1 Stevenson DD, Simon RA *et al.* Sensitivity to aspirin and nonsteroidal anti-inflammatory drugs. In: Middleton E,

Induction of Therapeutically Relevant Cytotoxic T Lymphocytes in Humans by Percutaneous Peptide Immunization

Hiroaki Yagi,[1] Hideo Hashizume,[1] Takahiro Horibe,[1] Yasushi Yoshinari,[1] Maki Hata,[1] Akihiro Ohshima,[1] Taisuke Ito,[1] Masahiro Takigawa,[1] Akihiko Shibaki,[2] Hiroshi Shimizu,[2] and Naohiro Seo[1]

[1]Department of Dermatology, Hamamatsu University School of Medicine, Hamamatsu, Japan and [2]Department of Dermatology, Hokkaido University Graduate School of Medicine, Sapporo, Japan

Abstract

Percutaneous peptide immunization (PPI) is a simple and noninvasive immunization approach to induce potent CTL responses by peptide delivery via skin with the stratum corneum removed. After such a barrier disruption in human skin, epidermal Langerhans cells, although functionally matured through the up-regulation of HLA expression and costimulatory molecules, were found to emigrate with a reduced number of dendrites. $CD8^+$ populations binding to MHC-peptide tetramers/pentamers and producing IFN-γ appeared in the blood after PPI with HLA class I–restricted antigenic peptides. PPI with melanoma-associated peptides reduced the lesion size and suppressed further development of tumors in four of seven patients with advanced melanoma. These beneficial effects were accompanied by the generation of circulating CTLs with *in vitro* cytolytic activity and extensive infiltration of tetramer/pentamer-binding cells into regressing lesions. PPI elicited neither local nor systemic toxicity or autoimmunity, except for vitiligo, in patients with melanoma. Therefore, PPI represents a novel therapeutic intervention for cancer in the clinical setting. (Cancer Res 2006; 66(20): 10136-44)

Introduction

Dendritic cell (DC)-based immunotherapy for cancer and infection is feasible, safe, and effective in some cancer patients when appropriately matured and activated DCs are administered (1–11). However, because of the lack of standardization in methods for *in vitro* generation of DCs and protocols to administer these vectors, comparison of clinical efficacy among DC immunotherapies, and thus, designing large clinical trials seems to be difficult (12). More critically, the intricate processes involved are costly and time-consuming, constituting an obstacle to clinical application of DC-based strategies. Targeting DCs should be ideally done *in vivo* (12, 13).

Epidermal Langerhans cells (LC), immature DCs residing in the outermost layer of the skin, become potent antigen-presenting cells (APC) after appropriate stimulation (14, 15). Because of their unique anatomic localization and immune functions, LCs are very attractive vectors for vaccine delivery (14, 16–19). Percutaneous peptide immunization (PPI) represents a novel immunotherapy using LCs as vectors for delivering all classes of peptide to the immune system. Removal of the stratum corneum (SC), the most superficial layer of the epidermis, by physical means, is essential in this simple and noninvasive method (20). The barrier removal process not only enhances the permeability of antigenic peptides applied to the skin but also matures LCs for antigen presentation (21). Following migration from barrier-disrupted skin to lymphoid organs, LCs bearing peptides induce potent CTL responses. Experiments in murine tumor models have shown that this simple and safe procedure is highly effective for prophylaxis and therapy of infection and tumors (19, 20, 22). The present study was designed to validate PPI as a clinical intervention for the management of malignancies in humans.

Materials and Methods

Human Subjects

A total of eight healthy males, with ages ranging from 24 to 56 years, and eight patients with stage III/IV melanoma (P1-P8; Table 1) were enrolled in the present study. Three healthy males, designated N1 (age, 35 years), N2 (40 years), and N3 (30 years), all having HLA-A*0201, underwent PPI with HIV gag peptides. Another six healthy subjects, with ages ranging from 24 to 56 years, participated in clinical and immunohistochemical studies following the removal of SC but did not receive PPI. Patients with melanoma received PPI with melanoma-associated antigenic peptides. Eligible criteria for PPI in the patients were: biopsy-proven American Joint Committee on Cancer stage III/IV melanoma; age, ≥20 years; Eastern Cooperative Oncology Group performance status, ≤1 on entry of PPI; HLA-A*0201 and/or HLA-A*2402 phenotype; normal blood CD4 and CD8 T cell numbers by flow cytometry; and normal quantitative immunoglobulin levels. Exclusion criteria were: prior chemotherapy or application of biologicals ≤4 weeks before trial entry, untreated lesions in the central nervous system, bulky hepatic metastatic lesions, pregnancy, and concurrent corticosteroid/immunosuppressive therapy. Patients with generalized inflammatory skin disease, autoimmune disease, or active infections, including viral hepatitis, were also excluded. P1 to P4, P7, and P8 developed metastatic lesions despite initial treatment involving wide local excision and therapeutic lymph node dissection followed by postoperative combination adjuvant therapy (23). P6 developed primary esophageal melanoma. Due to resection of all the skin lesions and metastatic lymph nodes, P1 was free from measurable lesions on entry and served for evaluation of CTL induction only. In contrast, due to the presence of measurable lesions on entry, both CTL induction and early clinical outcome were assessed in P2 to P8.

In all subjects, routine blood examinations including a hemogram, and assessment of liver and renal function and autoantibodies showed no abnormalities on entry to PPI treatment. Serologic tests for HIV were negative, whereas serum hemagglutination inhibition titers for influenza A virus showed positive results. This study was approved by the institutional

Note: H. Yagi and H. Hashizume contributed equally to this work.

Requests for reprints: Hiroaki Yagi, Department of Dermatology, Hamamatsu University School of Medicine, 1-20-1 Handayama, Hamamatsu 431-3192, Japan. Phone: 81-53-435-2303; Fax: 81-53-435-2368; E-mail: hiroyagi@hama-med.ac.jp.

doi:10.1158/0008-5472.CAN-06-1029

review board. Informed consent was obtained from all participants according to the Declaration of Helsinki.

Synthetic Peptides and Reagents

Three custom-synthesized peptides including HIV gag (SLYNTVATL), influenza A matrix protein (MP; GILGFVFTL; American Peptide Company, Inc., Sunnyvale, CA), and modified Melan-A immunodominant cells (ELAGIGILTV; Peptide Institute, Inc., Osaka, Japan; ref. 24), were used as HLA-A*0201-restricted epitopes and four custom-synthesized peptides including MAGE-2 (EYLQLVFGI), MAGE-3 (IMPKAGLLI), gp-100 (VWKTWGQYW), and tyrosinase (AFLPWHRLF; Peptide Institute) were used as HLA-A*2402-restricted epitopes. Their purity was >95.0% as confirmed by high-pressure liquid chromatography. Phycoerythrin (PE)-labeled MHC tetramers specific for the HIV gag and Melan-A peptides were purchased from Beckman Coulter (Villepinte, France) and PE-labeled MHC-pentamers for MAGE-2, MAGE-3, and tyrosinase were custom-synthesized by ProImmune Limited (Littlemore, United Kingdom). The monoclonal antibodies (mAb) used in this study were anti-S-100 protein (DAKO, Glostrup, Denmark), anti-DC-LAMP/CD208 (Beckman Coulter), anti-Langerin/CD207 (Vector, Burlingame, CA), PE-labeled or PerCP-labeled anti-HLA-DR, FITC-labeled anti-CD4, PE-labeled or PerCP-labeled anti-CD8 and PerCP-labeled anti-CD45 (BD Biosciences, San Jose, CA), PE-labeled anti-CD1a, FITC-labeled anti-HLA-ABC (pan-HLA class I), anti-CD80, and anti-CD86 (PharMingen, San Diego, CA). RPMI 1640 complete was used for culture medium (20).

Epidermal Barrier Disruption

To remove SC, 5 × 5 cm square plastic plates were painted evenly with ~100 mg/plate of cyanoacrylate (Aron alpha A, Sankyo, Japan), tightly attached to the skin for 3 minutes and removed gently. This procedure was repeated thrice at one spot.

Transepidermal Water Loss Evaluation

Transepidermal water loss (TEWL) was measured using a Tewameter TM210 (Courage + Khazaka Electronic GmbH, Köln, Germany) as previously described (21).

PPI

Solutions of immunization peptides were made immediately before use. HLA-A*0201 subjects received 10 mg of HIV gag peptide in 10 mL of PBS or 16 mg of Melan-A peptide in 8 mL of 5% DMSO in PBS (5% DMSO). A cocktail of 5 mg each of MAGE-2, tyrosinase, and gp-100 peptides in 10 mL of PBS, and 4 mg of MAGE-3 peptide in 2 mL of 5% DMSO, were used for HLA-A*2402 subjects. These concentrations represented the saturation points of the peptides at room temperature. In P3 and P8, who had both HLA-A*0201 and HLA-A*2402, the MAGE-3 peptide solution contained 4 mg of Melan-A peptide. Twenty-four hours after the removal of SC, these peptide solutions were soaked up by gauze pads (each 5 × 5 cm) and applied to four barrier-disrupted areas (total area, 100 cm^2) of HLA-A*0201 subjects and to the six areas (total area, 150 cm^2) of both HLA-A*2402 subjects and individuals with both alleles. The pads were immediately covered with a film dressing and removed 24 hours later. PPI was repeated six times in normal volunteers and seven times in patients with melanoma at monthly intervals by placing the patches at different sites of the arms, thighs, abdomen, and back. Assessment of hemograms, and liver and renal functions was done 1 week following each PPI and at 1- to 3-month intervals thereafter.

Skin Specimens and Epidermal Cell Suspensions

Biopsy specimens were processed for routine histology and immunohistochemistry (25). The epidermal sheets were separated from the dermis in 0.02 mol/L of EDTA-PBS at 4°C for 18 hours and subjected to immunohistochemical staining. Epidermal suspensions were prepared from blister roofs by limited trypsinization (26).

Identification of LCs

Cells expressing S-100 protein in epidermal sections, and those positive for HLA-DR and CD1a in epidermal sheets and suspensions were identified as LCs (14, 27). Immunostained epidermal sheets were observed in a confocal laser scanning microscope (MRC-600; Bio-Rad, Hercules, CA; ref. 27). Epidermal cell suspensions were stained with a PE-labeled anti-CD1a mAb, a PerCP-labeled anti-HLA-DR mAb, and any one of an FITC-labeled anti-HLA-ABC mAb, an FITC-labeled anti-CD80 mAb, an FITC-labeled anti-CD83 mAb, an FITC-labeled anti-CD86 mAb, or FITC-labeled control antibodies and subjected to flow cytometry.

Flow Cytometry

Samples were run on a FACSCalibur flow cytometer (BD Biosciences) using CellQuest Software as described (28, 29). Three × 10^4 and 2 × 10^5 events were analyzed for epidermal samples and blood cells, respectively. For analysis of the epidermal samples, only size gates were used for counting the total number of HLA-ABC$^+$ epidermal cells. Gates for LCs were set as described in the legend for Fig. 1.

Measurement of Immune Responses

Peripheral blood mononuclear cells (PBMC) were purified before and 7 days after each PPI by standard Ficoll density centrifugation and subjected to flow cytometric analysis for cell surface staining and intracellular IFN-γ expression. Because binding to tetramers and pentamers and IFN-γ staining are highly reproducible with a variation of <5%, when the number of positive cells was +2 SD above the mean background staining, we defined this as the specific induction of antigen-specific CTLs.

Cell culture. PBMCs (5 × 10^6 cells/well in complete medium in 12-well tissue culture plates) were stimulated with immunization peptide (10 μg/mL), influenza A MP (10 μg/mL), or Con A (1 μg/mL; Sigma-Aldrich, St. Louis, MO) for 5 days and underwent either tetramer or pentamer staining and *in vitro* cytotoxic assay. Alternatively, cells cultured for 48 hours were subjected to intracellular IFN-γ production. Control cultures contained no stimulant. PBMCs from HLA-A*0201 or HLA-A*2402 subjects without PPI were cultured under identical conditions.

MHC tetramer and pentamer staining. Fresh or cultured PBMCs were stained with PE-labeled HLA-A*0201 tetramers or PE-labeled HLA-A*2402 pentamers and a gating kit (Beckman Coulter) according to the manufacturer's directions.

Intracellular IFN-γ analysis. GolgiStop (0.7 μL/mL, PharMingen) was added to cultures 8 hours before harvesting. Cells were reacted with a PerCP-conjugated anti-CD8 mAb, permeabilized in CytoFix/Cytoperm plus Perm/Wash buffers (PharMingen), and stained with an FITC-labeled anti-IFN-γ mAb (PharMingen). Control levels were determined with an appropriate isotype-matched antibody in each experiment.

***In vitro* peptide-dependent cytotoxic assay.** Only cultures containing >5% of tetramer-positive or pentamer-positive cells among CD8$^+$ cells following peptide stimulation were further expanded with rIL-2 (10 units/mL) for 3 days for effector cells. T2-A24 target cells (1 × 10^6 cells; T2 cell line transfected with HLA-A*2402 gene; ref. 30) incubated with immunizing peptide at 1 μg/mL for 1 hour were subjected to both HLA-A2-restricted and HLA-A24-restricted, calcein-AM release CTL assays (Dojindo Lab., Kumamoto, Japan). Briefly, T2-A24 cells were labeled with 5 μmol/L of calcein-AM in serum- and phenol red–free Iscove's modified Dulbecco's medium (IMDM; Invitrogen Co., Carlsbad, CA) at a concentration of 2 × 10^6 cells/mL for 40 minutes. Effector and target cells in 200 μL of IMDM supplemented with 10% FCS were distributed into U-bottomed 96-well microtiter plates at effector/target ratios of 2, 5, and 10. After incubation at 37°C for 3 hours, the concentration of calcein-AM in the medium was measured in a fluorescence analyzer (Synergy HT, Bio-Tek Inst., Inc., Winooski, VT). Maximal lysis was determined by adding lysis buffer to target cells and percentage-specific lysis were calculated as described previously (31).

Therapeutic PPI and Assessment of Early Clinical Outcome

Based on the kinetics of CTL generation in the blood, we instituted a treatment plan of PPI for patients with melanoma consisting of immunization with melanoma-associated peptide, seven times in total, done once a month. All baseline evaluations were done on entry. Tumor responses and side effects were assessed based on physical examination and laboratory investigation after completion of PPI. To assess tumor responses, the size of target lesions selected according to the Response Evaluation Criteria in Solid Tumors guidelines (32) was measured before and after PPI. Imaging-based evaluations were analyzed using NIH Image software for digital images. In P8, the dot densities in ^{99m}technetium

Table 1. Patient characteristics, disease status on entry and after PPI, and immunologic and clinical responses to PPI

Patient ID*	Age/gender	HLA-A		Stage/months after staging/previous therapy	Status/measurable disease on entry/number of target lesions	% $CD3^+$ $CD8+$ T cells in peripheral blood †	Number of peptide-specific T cells/10^4 $CD8^+$ cells in pre-PPI/post-PPI blood samples	
		02/01	24				Melan-A ‡	Tyrosinase ‡
P1	53/F	+	–	Stage IV/48/surgery, DAV-feron	CR/surgical removal of all skin and LN lesions/0	20.4	2/36	ND
P2	78/F	–	+	Stage III/7/surgery, DAV-feron	PD‖/surgical removal of all skin and LN lesions/0	19.8	ND	12/53
P3	77/M	+	+	Stage IV/20/surgery, DAV-feron	PD/mediastinal LN mass by CT and ^{67}Ga scintigraphy/1	16.8	2/94	11/61
P4	20/M	–	+	Stage IV/7/surgery, DAV-feron	PD/skin, lung and liver nodules by CT and MRI/10	27.2	ND	19/22
P5	68/F	–	+	Stage IV/5/surgery	PD/s.c. nodules by CE and CT/5	21.7	ND	15/14
P6	52/M	–	+	Stage III/2/none	PD/esophageal mass by CT and endoscopy/1	20.5	ND	6/105
P7	63/M	+	–	Stage IV/6/surgery, DAV-feron	PD‖/s.c. nodule by CE/1	24.2	1/118	ND
P8	77/M	+	+	Stage IV/5/surgery, DAV-feron	PD/multiple bone metastases by ^{99m}Tc bone scintigraphy/6	17.2	4/113	9/75

Abbreviations: CE, clinical examination; CR, free from melanoma for >4 weeks before entry; CT, computed tomography; DAV-feron, adjuvant therapy with i.v. dacarbazine, nimustine hydrochloride, and vincristine plus lesional injection of IFN-β; LN, lymph node; MRI, magnetic resonance imaging; PD, progression of measurable disease and/or new lesions; ND, not done.

*Patient ID, patient identification number.

† Percentages after lymphocyte gating by flow cytometry.

‡ Number of cells positive for MHC tetramers or pentamers/10^4 $CD8^+$ T cells in freshly isolated PBMCs.

§Number of intracellular IFN-γ-positive cells/10^4 $CD8^+$ T cells in PBMCs stimulated with gp-100 peptide (10 μg/mL) for 48 hours and subjected to an intracellular IFN-γ assay.

‖P2 and P7 developed new metastatic skin nodules at frequencies of one and three per 2 months, respectively, before entry.

¶In P4 and P5, the sums of the longest diameters for 10 and 5 lesions, respectively, were measured as the pre-PPI and post-PPI sums of the longest diameters.

**The dot densities in ^{99m}technetium hydroxymethylene diphosphonate bone scintigraphs of the metastatic lesions (indicated in Fig. 4) pre-PPI/post-PPI were 98.4/60.8 (#1), 128.6/59.8 (#2), 72.3/55.1 (#3), 84.3/71.3 (#4), 135.8/118.5 (#5), and 101.3/100.8 (#6). The serum 5-S-cysteinyldopa level reduced from 27 nmol/L pre-PPI to 4.2 nmol/L post-PPI (normal, <8.0 nmol/L).

hydroxymethylene diphosphonate bone scintigraphs were compared before and after PPI. The mean background density was calculated based on the density of three unaffected areas in a scintigraph. After the mean background densities before and after PPI were equalized, the lesional density was determined by analyzing the densities of square-framed areas representing bone metastasis.

Statistical Analysis

Student's t test was employed for comparisons, with $P < 0.05$ considered significant.

Results

Clinical observations after removal of sc. After removal of SC, faint and transient erythema developed in the treated sites which disappeared within 1 hour. Subjective symptoms such as pain or skin irritation during or after the manipulation were minimal or absent.

Kinetics of LCs in barrier-disrupted skin. Tissue histology revealed that 60% to 80% of the SC was removed in normal subjects ($n = 3$), on comparison of the thickness of SC before and immediately after barrier disruption, using adjacent skin as a control (Fig. 1*A*). TEWL values significantly increased from 8.10 ± 0.66 before manipulation to 16.83 ± 2.20 g/m^2/h after the removal of SC ($n = 3$, $P < 0.05$), indicating that considerable barrier disruption occurred with the method employed. Recovery was already evident at 48 hours and there were minimal or no inflammatory responses after 12, 24, and 48 hours as revealed by tissue histology. S-100^+ LCs showed larger cell bodies with fewer dendrites after the removal of SC compared with their

Table 1. Patient characteristics, disease status on entry and after PPI, and immunologic and clinical responses to PPI (Cont'd)

Number of peptide-specific T cells/10^4 $CD8^+$ cells in pre-PPI/post-PPI blood samples			Sums of the longest diameters of pre-PPI/post-PPI target lesions (cm)	Clinical outcome after PPI/side effects	Follow-up
MAGE-2[‡]	MAGE-3[‡]	gp-100[§]			
ND	ND	ND	0/0	No new lesions/generalized, progressive vitiligo	Disease-free for 19 months after PPI
6/68	9/106	6/30	0/0	No new lesions/none	Three new s.c. nodules (<5 mm in size) at 3 months after first round of PPI, which disappeared after the second round of PPI
8/42	14/212	4/23	3.2/0.9	Normal LN size/generalized, progressive vitiligo	Disease-free for 15 months after PPI
6/34	22/189	4/3	22/32[¶]	New metastatic lesions/none during PPI	Early death due to melanoma lesions
4/34	14/206	8/9	17/8[¶]	Decrease in size of target lesions/generalized, progressive vitiligo	New cutaneous and metastatic lesions developed despite continuous immunization for 13 months
8/93	8/204	12/243	4.0/5.5	Enlargement of a lesion/ generalized vitiligo	Death due to melanoma lesions at 4 months after PPI
ND	ND	ND	2/0	No new lesions/none	Two new s.c. nodules (<5 mm in size) at 5 months after first round of PPI, which disappeared after second round of PPI
18/41	16/94	5/75	Reduced intensities of the scintigraphy signals**	No new lesions/none	New lesion at 4 months after PPI despite unchanged densities of previous lesions

counterparts in intact skin. Both epidermis and dermis at 12 and 24 hours harbored $S\text{-}100^+$ cells, whereas most of them were located in the dermis at 48 hours. $HLA\text{-}DR^+$ cells were found to be larger and stained more brightly at 12 and 24 hours in epidermal sheets (Fig. 1*A, inset*) as compared with the intact skin case. At 48 hours, $Langerin^+$ cells were distributed in both epidermis and dermis, whereas $DC\text{-}LAMP^+$ cells were found mainly in the dermis. Enumeration of $CD1a^+$ cells in $HLA\text{-}ABC^+$ epidermal cell suspensions showed that essentially all LCs remained in the epidermis at 12 and 24 hours, and about half of this population migrated into the dermis at 48 hours (Fig. 1*B*). Enumeration of LCs in the epidermal sheets of three individuals showed that the mean number of $HLA\text{-}DR^+$ cells were 83% of the intact skin case at 24 hours and 39% of the cells remained in the epidermis at 48 hours. In accordance with these morphologic observations, the expression of HLA-ABC and HLA-DR (Fig. 1*C*) was up-regulated and the numbers of $CD80^+$, $CD83^+$, and $CD86^+$ (Fig. 1*D*) cells in LC populations were increased at 12 and 24 hours. The cells expressing CD86 remained increased in number even at 48 hours. Fully mature LCs are recognized by their strong surface expression of MHC class I/class II, CD80, CD86 costimulatory molecules, and CD83 maturation markers (33). Therefore, these findings indicated LC subpopulations to be activated *in situ*, then emigrating from the epidermis following disruption of the epidermal barrier by removal of SC.

Induction of antigenic peptide-specific CTLs by PPI. Based on the LC kinetics, we reasoned that optimal CTL priming might be induced by the application of antigenic peptides 24 hours after barrier disruption and subsequent exposure of the skin sites to the peptides for 24 hours. Normal subjects (N1, N2, and N3) received PPI with the HIV gag peptide. Six patients with stage IV melanoma (P1, P3, P4, P5, P7, and P8) and two patients with stage III melanoma (P2 and P6) underwent PPI with melanoma-associated antigenic peptides. Application of peptide at SC-removed sites was well tolerated, without local reactions such as irritation, redness and erosion, or systemic toxicity evidenced by rashes, fatigue, or fever. None of the study participants experienced lymphadenopathy thought to be related to PPI.

The appearance of CTLs was assessed periodically in the peripheral blood with reference to cells positive for tetramers and pentamers and intracellular $IFN\text{-}\gamma^+$ cells. Representative data of CTL induction in normal subjects and melanoma patients are shown in Figs. 2 and 3. Tetramer/pentamer-positive $CD8^+$ T cells were successfully detected in freshly obtained blood when assayed 7 days after the fourth immunization with HIV gag in cases N1 to N3, and after the fifth to sixth immunization with melanoma-associated peptides in patients P1 to P3 (Fig. 2*A-C*). The frequencies of binding cells were maintained in N1 and N2, whereas frequencies were increased in N3, P1, P2, and P3 following repeated immunization. Such *in vivo* expansion of CTL in normal individuals and patients with melanoma was antigen-specific because tetramer-binding responses were apparently enhanced in cultures stimulated with immunizing peptide but not with nonimmunizing peptide (Fig. 2*D*). The generation of HLA-A*0201-restricted CTLs was also detected with Melan A-specific tetramers in P7 and P8. After completion of therapeutic PPI, P2, P3, P6, P7, and P8 developed $CD8^+$ T cells reactive with pentamers for tyrosinase, MAGE-2, and MAGE-3, whereas only MAGE-2-specific

and MAGE-3-specific binding occurred in P4 and P5 (Table 1). Application of the HIV gag peptide to intact skin for 24 hours done once a month for five times did not induce CTL responses in N1 and N2. These data clearly indicate that repeated immunization induces and maintains antigenic peptide-specific CTLs.

Antigenic peptide-specific production of intracellular IFN-γ. Stimulation with Con A and Melan-A peptide induced significant numbers of intracellular IFN-γ^+CD8^+ T cells in patients undergoing PPI (Fig. 3*A*). PPI induced $CD8^+$ T cells with intracellular IFN-γ after the fifth immunization with the HIV gag in N1 to N3, and after the sixth and fourth immunization with Melan-A in P1 and P3, respectively (Fig. 3*B*). In addition, $CD8^+$ T cells positive for intracellular IFN-γ were expanded after stimulation *in vitro* with influenza A MP in HLA-A*0201-positive participants who were revealed to have functional antibodies for influenza A viruses by serologic studies. These observations not only indicated the presence of functional CTLs in the peripheral blood but also confirmed the feasibility of the present assay for detecting IFN-γ-producing cells. Four of six HLA-A*2402-positive melanoma patients (P2, P3, P6, and P8) developed gp-100-specific T cells positive for intracellular IFN-γ at completion of therapeutic PPI (Table 1). Therefore, we concluded that repeated immunization in PPI induces and maintains immunologically active, peptide-specific CTLs.

***In vitro* cytolytic function of PPI-induced CTLs.** In cytotoxic assays at completion of PPI, PBMCs from P2, P3, and P5 exerted a marked antigen-specific killing activity against HLA-A*2402 peptide-pulsed T2-A24 cells. Figure 3*C* shows the results of representative experiments with tyrosinase in P2. Effector cell populations contained 8.2%, 7.3%, and 6.7% peptide-matched pentamer-positive cells among $CD8^+$ cells in P2, P3, and P5, respectively. Optimal killing activity was observed with tyrosinase in P2, MAGE-2 in P3 (99.7 ± 5.9%, $P < 0.01$ compared with control; 56.2 ± 2.5%), and MAGE-3 in P5 (80.6 ± 3.4%, $P < 0.01$ compared with control; 54.6 ± 0.9%) at an effector-to-target ratio of 10. P1 and P3 also showed killing activity against HLA-A*0201-restricted target cells pulsed with Melan-A peptide (data not shown). The cytolytic activity was always detected in cultures which successfully proliferated on stimulation with immunizing peptide. CTLs from P4 could not be expanded to the level necessary for killing assays. Therefore, the therapeutic efficacy of PPI seemed to be correlated with *in vitro* effective propagation of peptide-specific CTLs with apparent cytolytic function.

Clinical efficacy of PPI for melanoma treatment. A critical issue is the therapeutic potency of PPI-induced CTLs. Therefore, the tumor response associated with the first round of therapeutic PPI was evaluated in P3 to P8 who had measurable lesions (Table 1). In P3, an enlarged mediastinal lymph node due to metastasis of melanoma cells decreased in size, from the longest diameter of 3.2 cm before PPI, to 0.9 cm at completion of PPI (Fig. 4*A*). P5 showed a >50% reduction in the sums of the longest

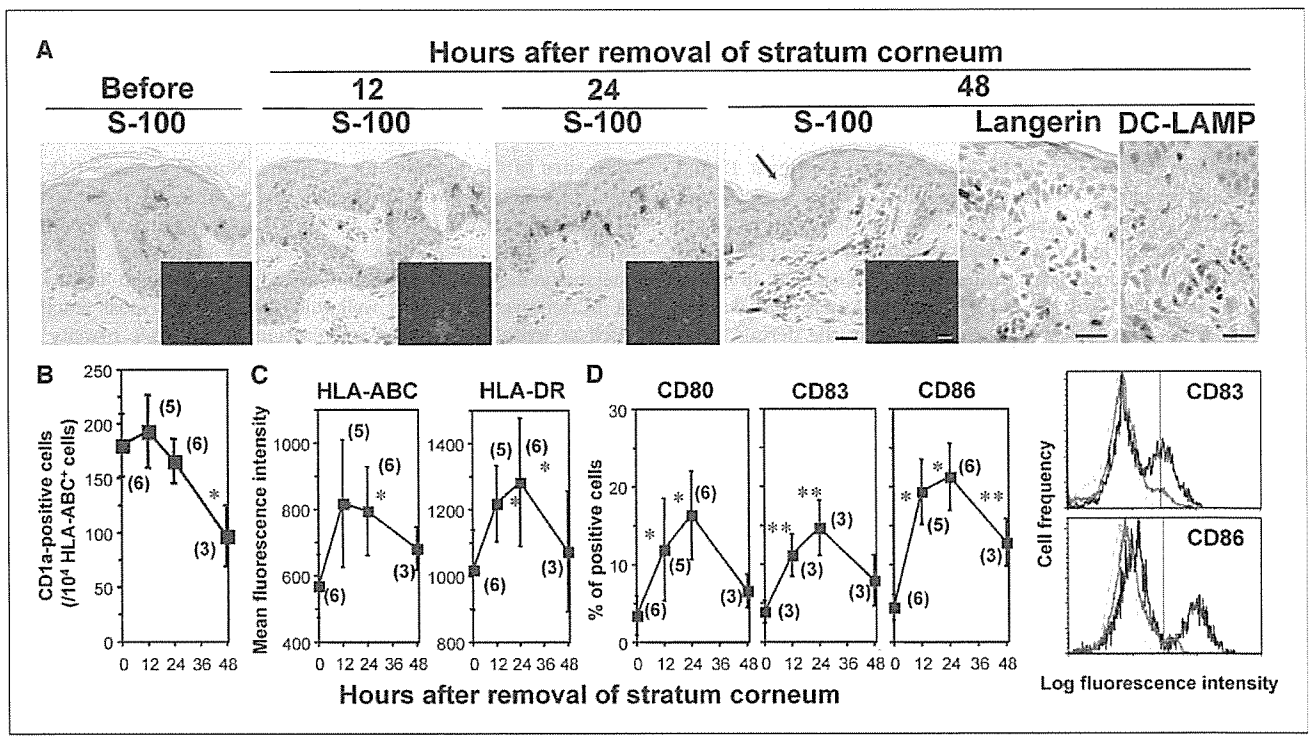

Figure 1. Kinetics of LCs and expression of HLA and costimulatory molecules on LCs in relation to removal of the SC. Skin samples from normal individuals were examined before, 12, 24, and 48 hours after removal of the SC. The numbers in parentheses indicate the number of subjects that participated. *A,* $S\text{-}100^+$, Langerin/$CD207^+$ and DC-LAMP/$CD208^+$ cells (*brown*) in the skin samples immunostained with a standard avidin-biotin complex method. Nuclear counterstaining was achieved with hematoxylin. *Arrow,* regenerating SC. *Insets,* composite confocal images of epidermal sheets showing $HLA\text{-}DR^+$ cells. Representative sections are shown. *Bar,* 50 μm. *B,* enumeration of $CD1a^+$ cells in $HLA\text{-}ABC^+$ epidermal cells. *Points,* mean; *bars,* ±SD. *C* and *D,* expression profiles of HLA-ABC, HLA-DR, CD80, CD83, and CD86 in epidermal LCs. *C*, mean fluorescence intensity was determined as a linear scale (0-1,020). *D,* percentage of positive cells in LC populations were determined. LCs were separated from contaminating epidermal cells using FL2-gate settings as PE-labeled $CD1a^+$ cells and FL3-gate settings as PerCP-labeled $HLA\text{-}DR^+$ cells, as well as forward scatter/side scatter gating. The viability of the cells within this gate was always >95% as determined by the addition of propidium iodide to each sample. Representative flow cytometric analyses of cell surface CD83 and CD86 expression before (*red lines*) and 24 hours after (*black lines*) the barrier disruption. Cells stained with isotype control antibody (*green lines*). *Points,* mean; *bars,* ±SD; *, $P < 0.01$; **, $P < 0.05$, as compared with no treatment (0 hours).

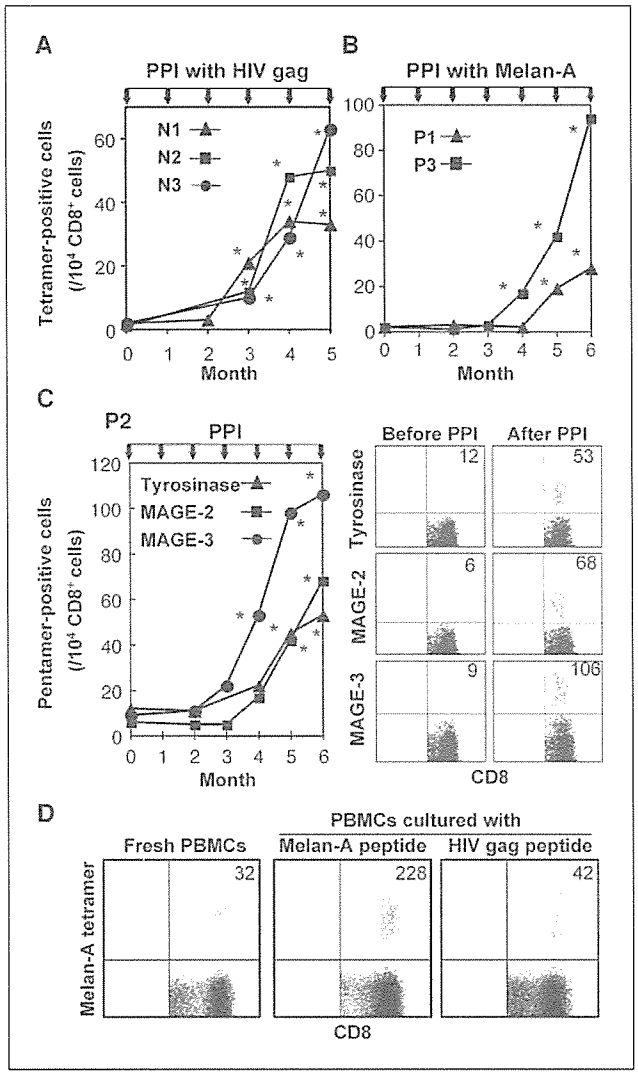

Figure 2. Induction of peptide-specific, tetramer-positive, and pentamer-positive $CD8^+$ T cells. PBMCs obtained 7 days after each PPI were immunophenotyped with the HIV gag-tetramer in N1 to N3 (*A*), Melan-A-tetramer in P1 and P3 (*B*), and pentamers for tyrosinase, MAGE-2, and MAGE-3 in P2 (*C*), and analyzed by flow cytometry. Alternatively, cells were cultured with Melan-A or HIV gag peptide for 5 days and subjected to tetramer binding assay (*D*). *A,* kinetics of HIV gag tetramer-positive cells. The value for HIV gag-specific cells/10^4 $CD8^+$ cells in HLA-A*0201 control subjects (n = 6) without PPI was 1.83 ± 0.75 (mean ± SD). *,+2 SD above the mean. *B* and *C,* kinetics of tetramer/pentamer-positive cells in melanoma patients. The number of Melan-A-specific cells/10^4 $CD8^+$ cells in HLA-A*0201 control subjects (n = 6) without PPI was 2.50 ± 1.05 (mean ± SD). The number of tyrosinase-, MAGE-2-, and MAGE-3-specific cells/10^4 $CD8^+$ cells in HLA-A*24 control subjects (n = 6) without PPI were 10.2 ± 5.9, 11.3 ± 5.0, and 15.6 ± 3.8, respectively (mean ± SD). *,+2 SD above the mean. *D,* specificity of tetramer-positive cell induction by PPI. Results of a representative experiment for cells after the seventh immunization with Melan-A from P1. Numbers are tetramer-positive cells/10^4 $CD8^+$ cells. Tetramer-positive cells in cultures stimulated with nonimmunizing peptide were always below the mean +2 SD of control subjects (n = 6).

diameters of five target lesions selected before PPI (Fig. 4*B*). In P7, a small s.c. nodule, with the longest diameter at 2 cm, disappeared. In P8, the intensities of the scintigraphic signals in five of six multiple bone metastases were attenuated after PPI (Fig. 4*C*). In accordance with these findings, the level of serum 5-S-cysteinyl-dopa was reduced from 27 nmol/L before PPI to 4.2 nmol/L after PPI (normal, <8.0 nmol/L). In P4 and P6, the melanoma invasion progressed rapidly, despite CTL induction, and both patients died of the tumor within 4 months of PPI completion. In P2 and P7, although skin nodules had developed at frequencies of one and three per 2 months, respectively, and been dissected during the 6 months prior to PPI, new lesions did not appear for 6 months during PPI. These patients developed several new lesions at

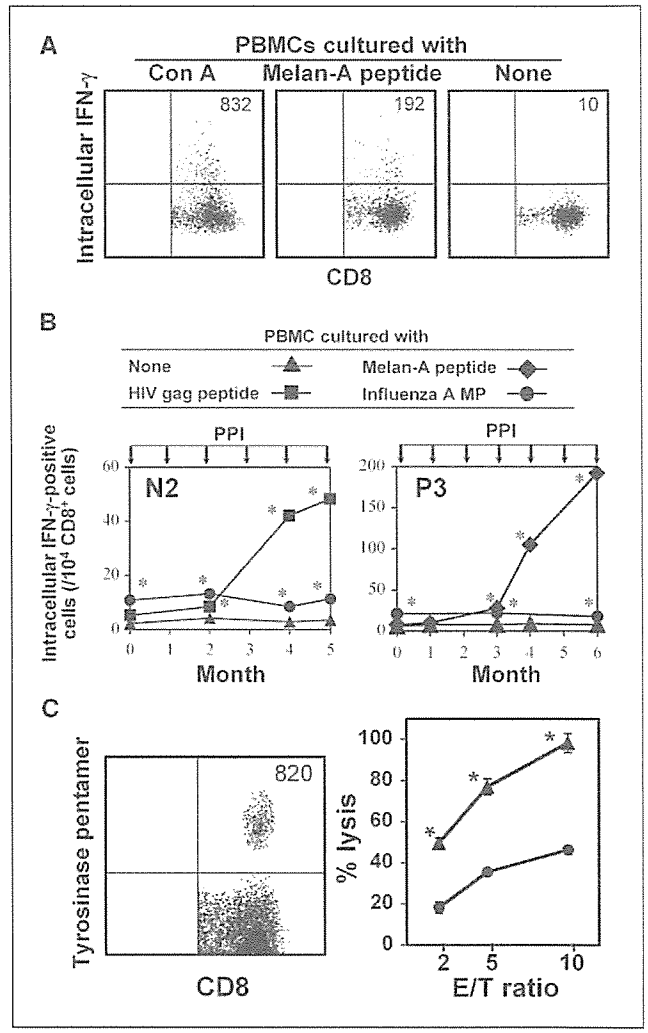

Figure 3. Induction of an intracellular IFN-γ^+ $CD8^+$ T cell response by PPI. PBMCs obtained 7 days after PPI were cultured with either HIV gag, Melan-A, influenza A MP, or Con A for 48 hours depending on the experiment purpose and subjected to intracellular IFN-γ assay. *A,* specific induction of intracellular IFN-γ-positive cells by PPI. Results of a representative experiment in P3 after the seventh immunization. Numbers indicate IFN-γ^+ cells/10^4 $CD8^+$ T cells. In the Con A culture, these were 320 in N1, 343 in N2, 425 in N3, and 892 in P1. *B,* kinetics of peptide-specific T cells producing IFN-γ. Results of representative experiments in N2 and P3. Immunizing peptide was HIV gag in N2 and Melan-A in P3. The number of HIV gag–specific cells/10^4 $CD8^+$ cells in HLA-A*0201 control subjects (n = 6) without PPI was 3.86 ± 1.77 (mean ± SD). The number of Melan-A-specific cells/10^4 $CD8^+$ cells in HLA-A*0201 control subjects (n = 5) without PPI was 4.17 ± 1.60 (mean ± SD). *,+2 SD above the mean. *C,* results of representative *in vitro* peptide-dependent cytolytic experiments in P2. PBMCs at completion of PPI were stimulated with tyrosinase and subjected to CTL assay in the presence of T2-A24 target cells loaded with (▲) or without (●) the peptide. Effector cell populations contained 820 tyrosinase pentamer-positive cells/10^4 $CD8^+$ cells as shown in a flow cytometric profile. *Points,* mean of triplicate cultures; *bars,* ±SD. *, $P < 0.01$ as compared with lysis of T2-A24 cells not loaded with the relevant peptide. *E/T ratio,* effector-to-target ratio.

3 to 5 months after completion of PPI, once the number of circulating CTLs had dropped to less than half the peak value (data not shown). The fact that P2 and P7 were free from melanoma lesions for 9 to 11 months during and after PPI suggested the suppressive effect of this procedure on tumor development. Therefore, the clinical outcomes in this small pilot study clearly suggest the beneficial effects of PPI for patients with advanced melanoma.

Migration of CTLs into melanoma lesions after PPI. Skin tissue specimens were available in association with PPI for P2 and P4, and subjected to histologic and immunohistochemical examinations as well as flow cytometric analysis. In P4, in whom the melanoma progressed despite CTL induction in the blood, there was no lymphoid cell infiltration before or after PPI (Fig. 5*A*, *a*). In P2, the metastatic lesions contained no cellular infiltrate before the first round of PPI (Fig. 5*A*, *b*). This patient received a second round of PPI due to the development of three new lesions at 3 months after completion of the first round of PPI. After the second immunization in the second round, the regressing lesions showed marked lymphoid cell infiltration and apoptotic and necrotic melanoma cells (Fig. 5*A*, *c* and *d*). $CD8^+$ cells had infiltrated the tumor mass and $CD4^+$ cells were located at the periphery of the lesions (Fig. 5*A*, *e* and *f*). Flow cytometric analysis revealed that the tumor-infiltrating leukocytes contained $CD4^+$ cells and $CD8^+$ cells in equal proportions (Fig. 5*B*). Furthermore, 9.8%, 8.4%, and 12.7% of the cells among the $CD8^+$ tumor-infiltrating cells were positive for tyrosinase, MAGE-2, and MAGE-3 pentamers, respectively (Fig. 5*B*). The proportions of tyrosinase, MAGE-2, and MAGE-3 pentamer–positive cells in the circulation at this time were 0.42%, 0.52%, and 0.8% of the $CD8^+$ cells, respectively, indicating selective migration of peptide-specific CTLs into the melanoma lesions.

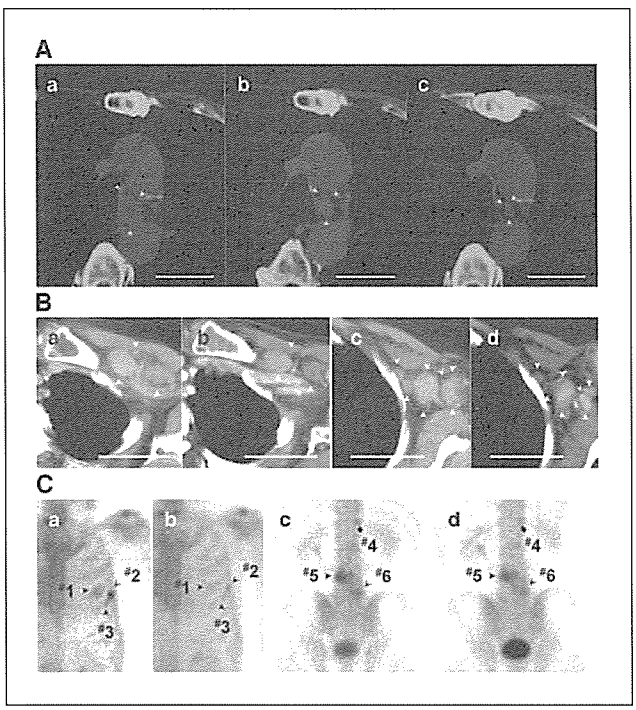

Figure 4. Clinical efficacy of PPI for melanoma treatment. *A*, computed tomography scans of a mediastinal lymph node (*arrowheads*) in P3 on entry (*a*), after the fourth PPI (*b*), and at completion of PPI (*c*). *B*, multiple metastatic lesions (*arrowheads*) in the left upper chest (*a* and *b*) and left axilla (*c* and *d*) in P5 on entry (*a* and *c*) and at completion of PPI (*b* and *d*). *C*, ^{99m}Tc-bone scintigraphs of metastatic bone lesions (#1-#6) in P8 before (*a* and *c*) and after (*b* and *d*) PPI. P3 presented with a melanoma lesion on the left palpebral conjunctiva and received orbital exenteration and wide local excision 15 years previously. Metastatic lesions appeared on the skin of the neck and the left parotid gland >12 years after the previous treatment. Despite total excision of the recurrent lesions and postoperative combination adjuvant therapy, metastases developed in mediastinal lymph nodes 3 months before entry. P5 underwent excision of primary skin lesions 5 years previously without any subsequent treatment, and developed multiple s.c. metastatic tumors at 5 months before entry. P8 had multiple bone metastases, as detected by bone scintigraphy, despite the resection of a lesion of the first toe of the right foot and right inguinal metastatic lymph nodes, and subsequent chemotherapy 2 years before entry.

Laboratory findings and untoward clinical features. Repeated assessment of hemograms and liver and renal functions revealed no abnormalities during and at completion of PPI in normal participants and the patients except P4. Results of the laboratory examination were normal during the 1-year follow-up period after completion of PPI in N1 to N3. Liver functions progressively deteriorated during PPI and until death in P4 because of multiple liver metastases. N1 to N3 developed no physical signs of autoimmunity, and rheumatoid factors or autoantibodies including antinuclear antibodies were negative 1 year after PPI. Generalized progressive vitiligo spots developed in P1, P3, P5, and P6 after several immunizations, although no other physical signs or serologic findings of autoimmunity were detected at completion of PPI.

Follow-up. P1 and P3 were disease-free for 15 to 19 months after the first round of PPI. New small s.c. nodules in P2 and P7, which developed at 3 and 5 months, respectively, after the first round of PPI, disappeared after a second round of PPI. Despite the regression of the initial target lesions at the end of PPI, P5 developed new s.c. and metastatic lesions while undergoing monthly immunization in succession to the PPI due to the patient's request. P8 developed a new bone lesion with an increase in the serum 5-S-cysteinyldopa level at 4 months after PPI, although the densities of the previous bone lesions remained decreased, as evaluated by scintigraphy.

Discussion

The present study showed that PPI, a novel immunization protocol for peptide application to barrier-disrupted skin, induces potent CTL responses and provides a promising approach for cancer therapy in human beings. Because an adjuvant effect seems to be inherent in perturbation of the skin integrity (21), the hallmark of PPI is that it closely mimics the natural trigger of DC activation, conducive to CTL expansion as fully activated effector cells. Although only a part (a maximum of 20%) of LCs were actually activated, the main and effective inducer of CTL would be LCs, considering their *in situ* kinetics after removal of SC in human and the augmented CTL priming capacity of LCs in barrier-disrupted murine skin (20). Recent studies in murine herpes virus infection models (34, 35), as well as novel mouse systems in which LCs can be selectively removed/ablated (36–38), have suggested that skin-resident APCs other than LCs contribute in the generation of immune responses *in vivo*. Therefore, it was possible that these cell types also participated in peptide-specific CTL immunity in the current protocol. Individual differences in the LC emigration profile of these APCs through skin and the amount of peptide absorbed via barrier-disrupted skin may be one critical factor in determining the timing and magnitude of CTL responses. An important issue is the demonstration of an actual therapeutic or preventive application of PPI in humans. In fact, the pilot study revealed a beneficial effect of PPI on the growth inhibition of